

Neuroendokriinsed tuumorid

When you hear hoofbeats, think horses, not zebras

...

When you hear hoofbeats, sometimes it's a ZEBRA.

Alina Kornejeva

v



Difuusne neuroendokriinrakude süsteem

- Tsentraalne grupp

Hüpotaalamus

Hüpofüüs

Epifüüs

- Perifeerne grupp

Kõrvalkilpnääre

Kilpnäärme C-rakud (medullaarne vähk)

Sümpaatiline närvisüsteem (paraganglioom)

Neerupealiste säsi (feokromotsütoom)

Pankrease Langerhansi saarekeste rakud

NE rakud

- Gastrointestinaal traktis (+ pankreas 70% NEN-dest)
- Bronhopulmonaalses süsteemis (25% NEN-dest)
- Urogenitaaltraktis
- Tüümuses
- Merckel rakud nahas



NET CANCER DAY

November 10

HOME	MEMBERSHIP	EDUCATION/CME	ENETS ANNUAL CONFERENCES	ENETS REGISTRY	RESEARCH
ABOUT US	ENETS GUIDELINES		GRANTS AND AWARDS	CENTERS OF EXCELLENCE	NET NURSE

CENTERS OF EXCELLENCE
About Centers of Excellence
CoE Interactive Map
CoE Programme Structure
How to apply as a CoE?
Annual Return Data
CoE Procedures
CoE Member Area
CoE Contact



Centers of Excellence (CoE) Interactive Map

The map shows numerous blue location pins across Europe, indicating the presence of Centers of Excellence. The right-hand side of the map features a scrollable list of countries, each with a right-pointing arrow. The countries listed are: Australia, Austria, Belgium, Denmark, France, Germany, Greece, Hungary, Ireland, Israel, Italy, Netherlands, Norway, Poland, Sweden, Uppsala, Switzerland, United Kingdom, and United States. The Uppsala entry includes a sub-entry: "Department of Endocrine Oncology, Uppsala University Hospital".

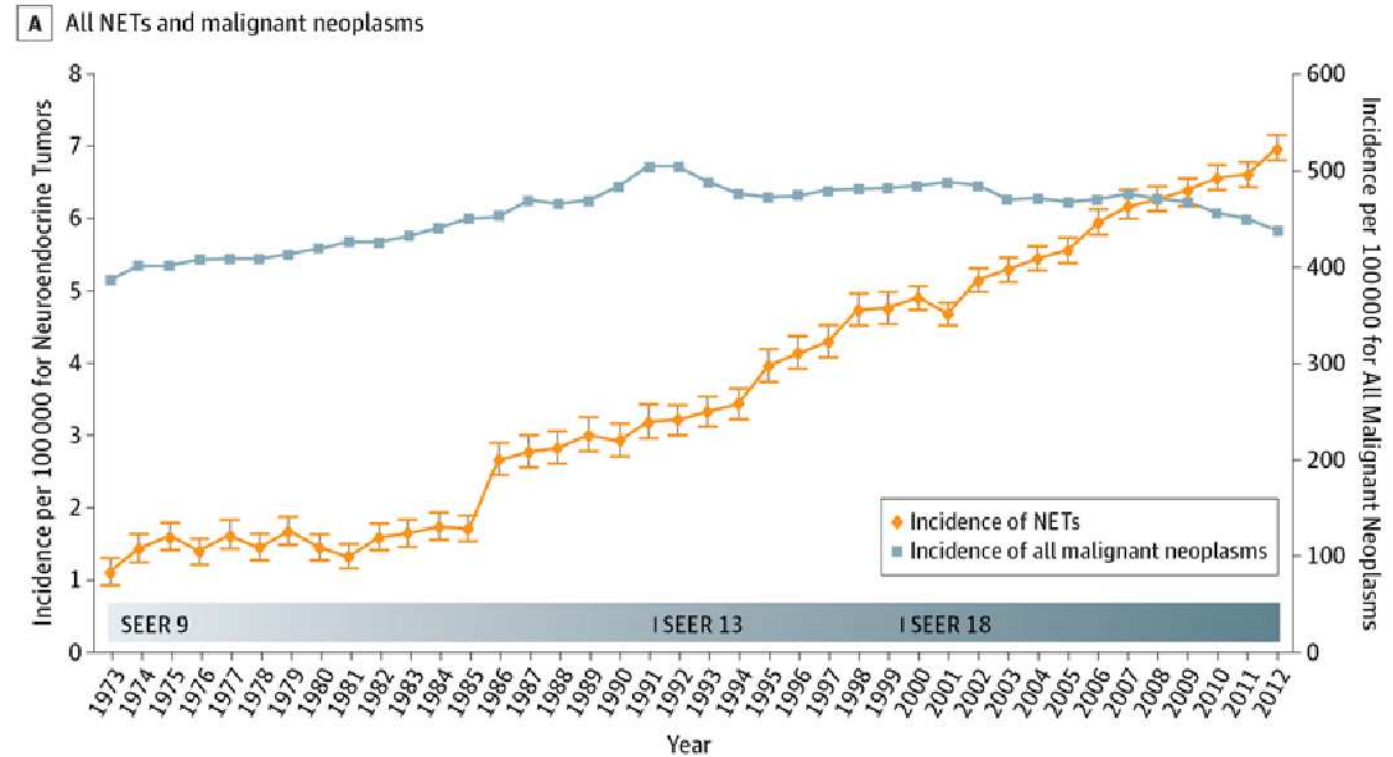


<https://www.enets.org/>

Epidemioloogia

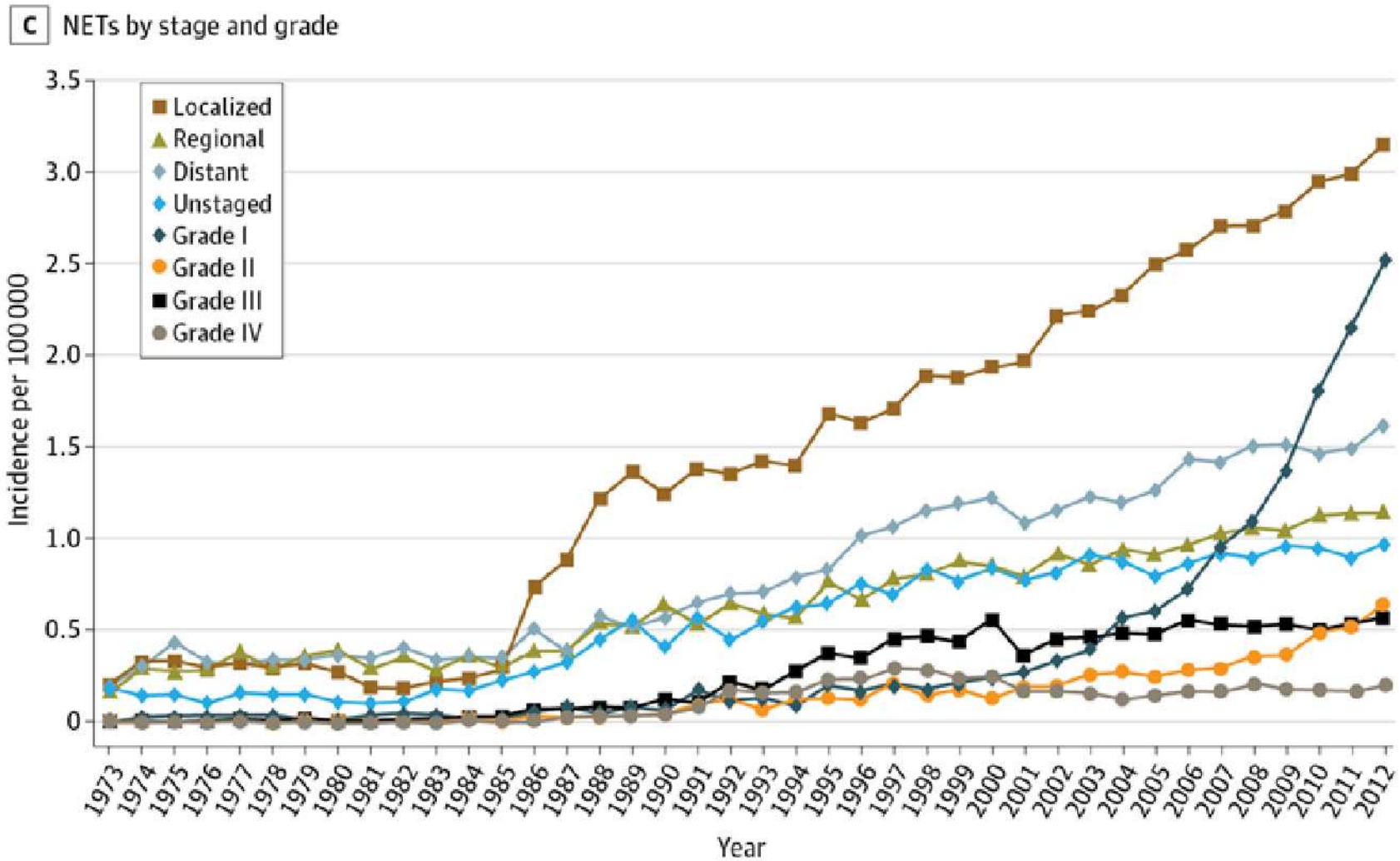
Taani andmed:

- autopsiate järgi 8,4/100 000 aastas
- Kopenhaageni riiklik haigla:
 - Haigestumus > 10 /100 000 aastas
 - Levimus > 50/100 000 aastas



Dasari, JAMA Oncology 2017, USA

Trends in the Incidence, Prevalence, and Survival Outcomes in Patients With Neuroendocrine Tumors in the United States



Dasari, JAMA Oncology 2017, USA

Elulemus

- 5 aasta elulemus NET keskus Kopenhaagen RH:
 - 76% peensoole NET puhul
 - 75% pankrease NET puhul (9% adenoCa puhul)

Radioloogia

- I/v kontrastainega KT, hilisarteriaalne - ja portovenosne faas
 - Klassika - arteriaalses faasis intensiivselt kontrasteeruv lesioon
- Peensoole NET ? - > CT enteroclysis - *fluoroscopic intubation-infusioon (via nasojejunal tube) small bowel examinations with abdominal CT*
- Pankreas/ duodenum - > endoskoopiline UH
- Maksa metastaasidele - > MRT

Mõisted

- NEN – neuroendokriine neoplaasia:
 - NET- neuroendokriine tuumor
 - NEC- neuroendokriine kartsinoom

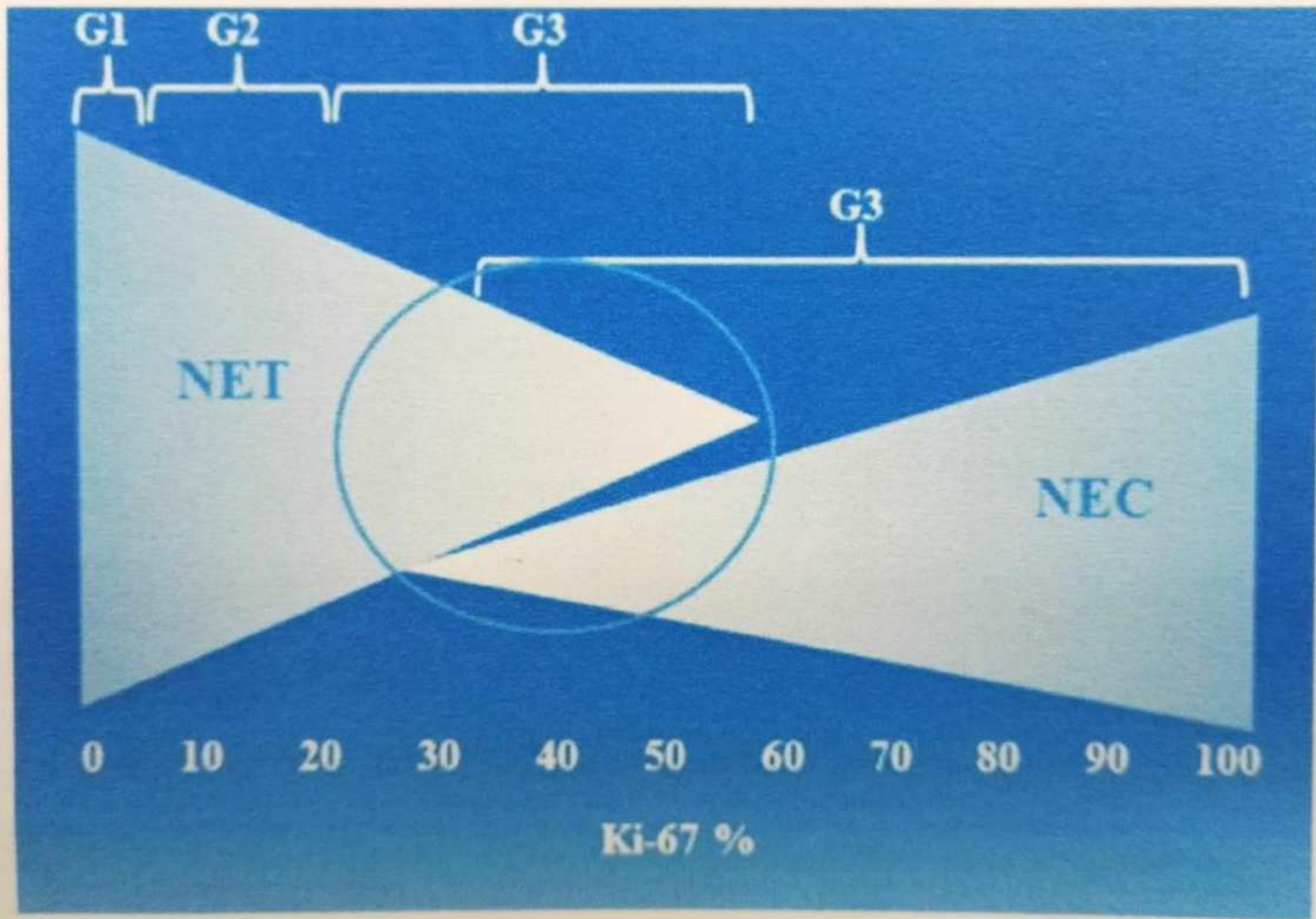
WHO 2019 klassifikatsioon, GI ja pankrease NEN

- G1: NET Ki-67* <3%
- G2: NET Ki-67 < 20%
- G3:
 - G3 NET Ki-67 > 20%
 - G3 NEC Ki-67 > 20%
 - *Large cell*
 - *Small cell*
- MiNEN – mixed neuroendocrine-non-neuroendocrine neoplasm(1/3 igat komponenti)

** The Ki-67 protein (also known as MKI67) is a cellular marker for proliferation, is encoded by the MKI67 gene. The name is derived from the city of origin (Kiel, Germany)*

Click & hold to compare

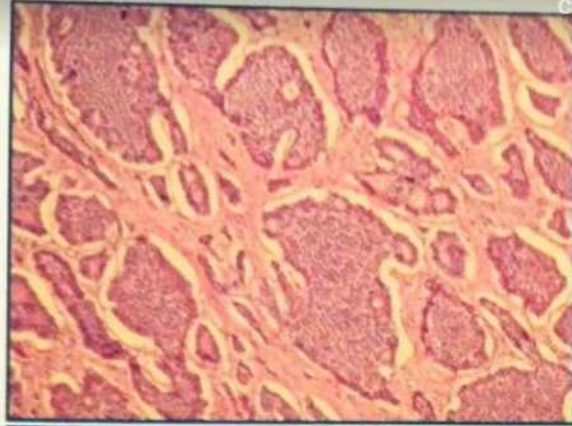
NEC and NET G3



Click & hold to compare



Insular

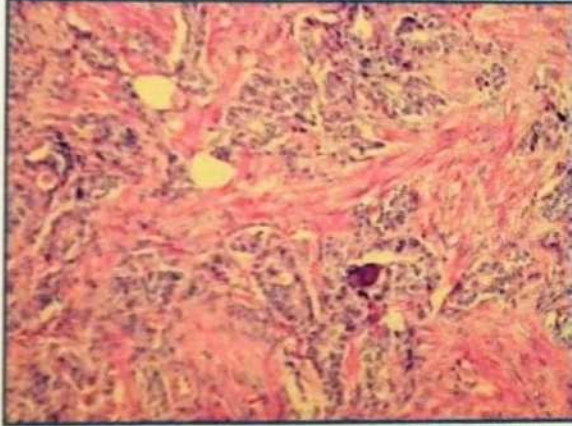


G
R
O
W
T
H

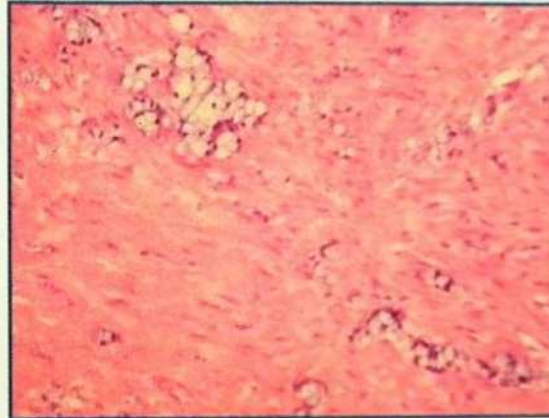


Rosettes

Glandular



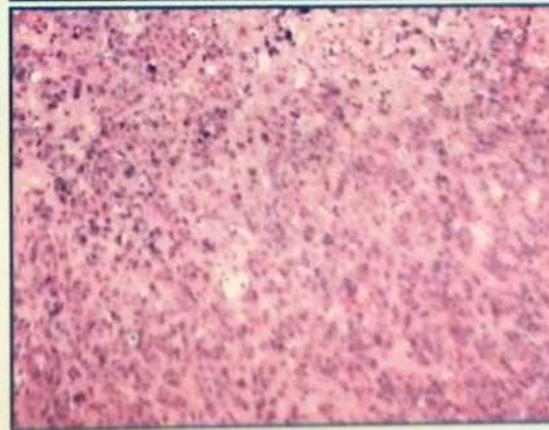
P
A
T
T
E
R
N
S



Goblet Cells

(now classified as
Goblet cell
adenocarcinoma)

Trabecular



Poorly
Differentiated
(NEC)

Click & hold to compare

NET-NET-TH
→ → NEC-adenoma CA
TM

For G3 tumours

P53

Rb1

ATRX/DAXX

PCR-NGS HS

50 most common mutations

PCR-MGMT

Methylguanine DNA methyl
transferase

For treatment with

Temozolomide

Teadamata algkolle, histoloogilised markerid

- TTF – kops?
- Somatostatiin – duodeenum, pankreas?
- Serotoniin – *midgut* ?

Kartsinoid

Kartsionoid tuumor – NET alaliik, *APUD* enterokromafiinsetest rakkudest GI ja bronhopulmonaalses süsteemis.

Kartsionoid sündroom – üleliigsest serotoniini produktsioonist kõige sagedamini GI kartsinoidist

8% patsientidest

Sümptomid:

Kõhulahtisus (80%)

Vasomotoorsed sümptomid – näo ja rindkere punetus

Südame parema poole puudulikkus (<15% fibroos-stenoos)

Bronhospasm (<10%)

Neuroendocrine neoplasms of the small intestine

Clinical manifestations

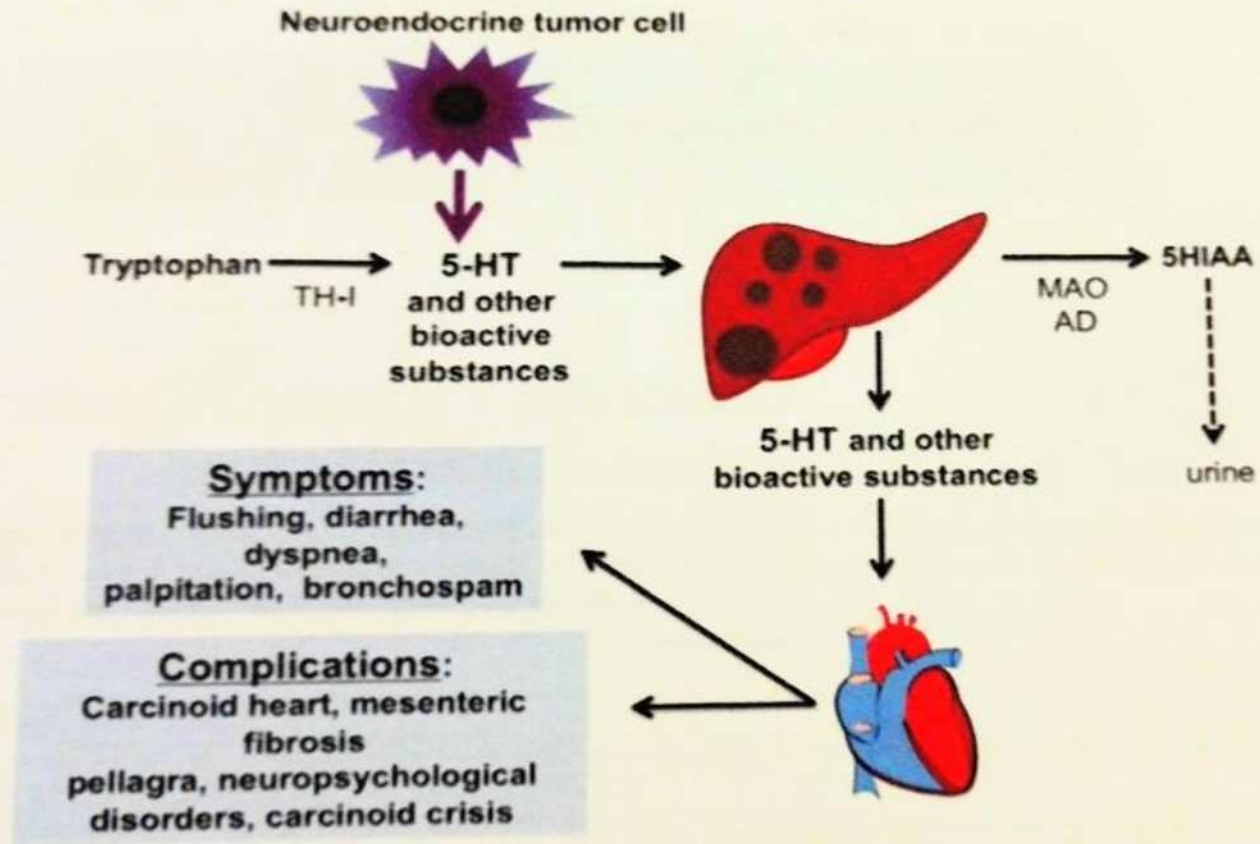
Related to metastatic and advanced disease

Carcinoid syndrome

- Incidence: 0.40 - 0.65 / 100.000 / year
- Caused by serotonin and peptides released from liver metastases to the major circulation
- Hormones released from the primary tumor to the portal venous circulation are metabolized by the liver and rarely cause carcinoid syndrome



Serotonin and carcinoid syndrome

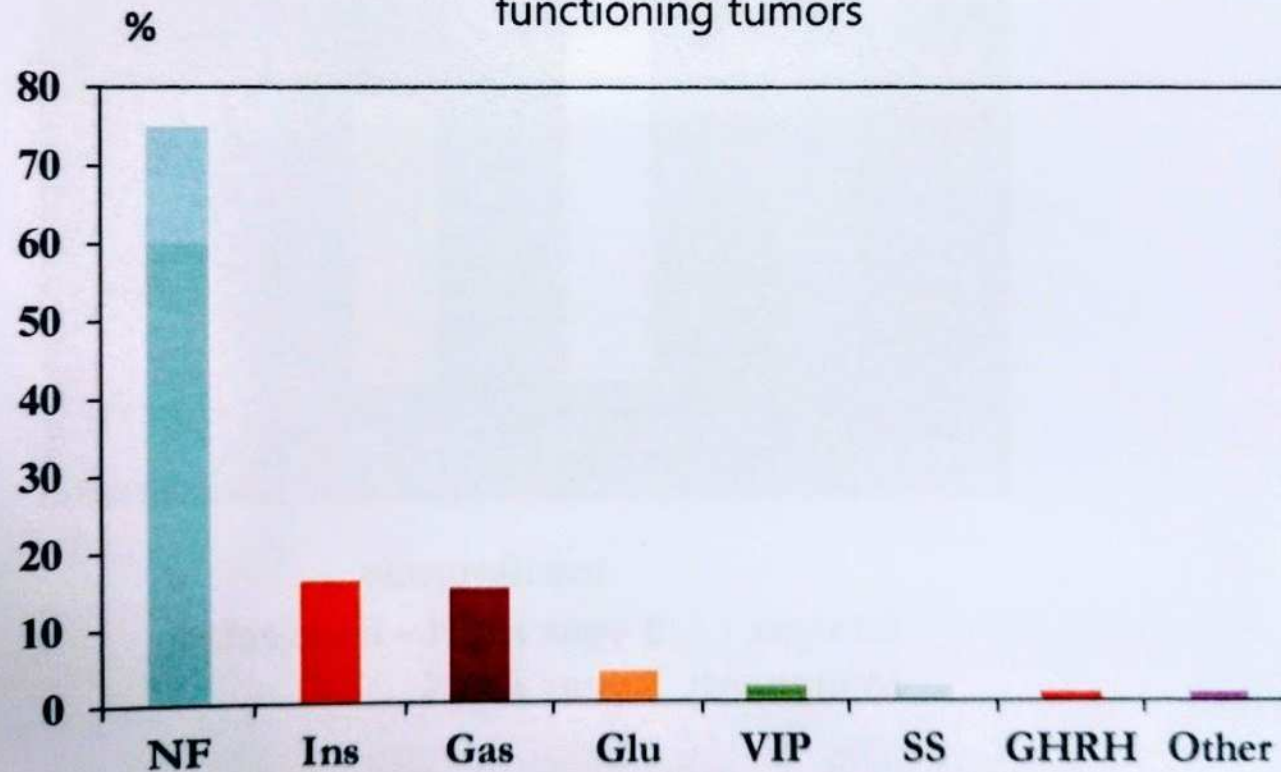


Abbreviations: 5-HT: serotonin; TH-I: tryptophan hydroxylase I; MAO: monoamine oxidase; AD: aldehyde dehydrogenase


Pancreatic NET

Incidence: 1/ 100.000 / year
Approximately 2 -10 % of pancreatic cancers

Distribution of non-functioning (NF) and
functioning tumors



Pancreatic Endocrine Tumors: Radiologic-Clinicopathologic Correlation

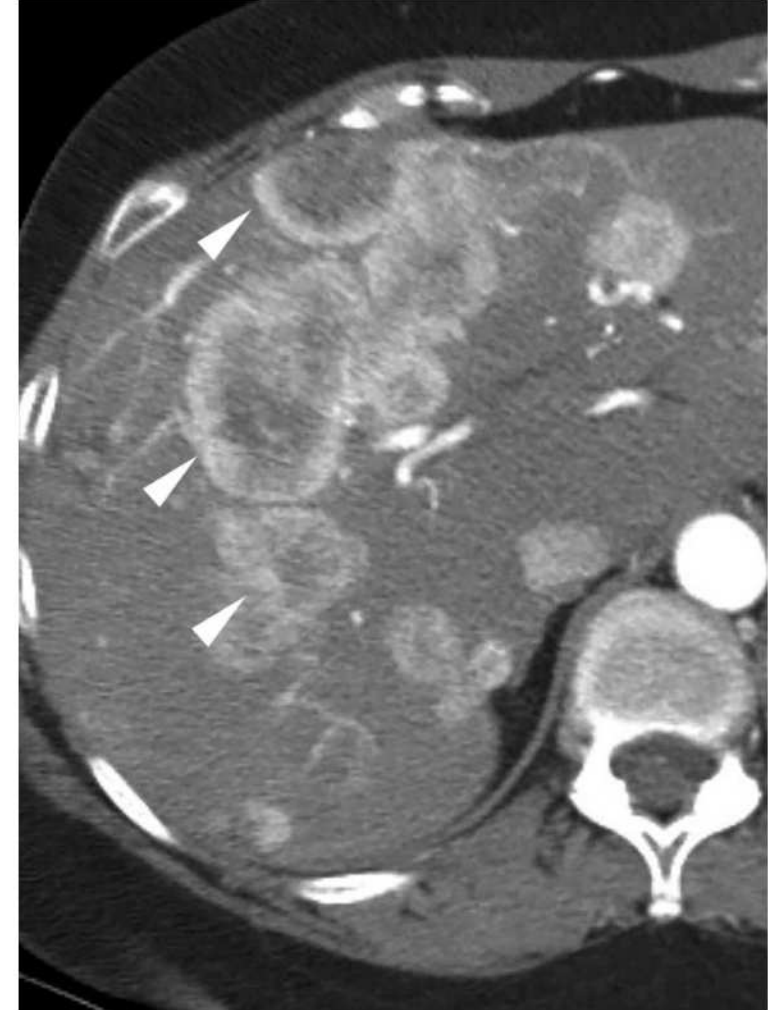
Rachel B. Lewis , Grant E. Lattin, Jr, Maj, Edina Paal



Axial contrast-enhanced CT image shows a well-defined mass in the pancreatic tail that demonstrates heterogeneous hyperenhancement.

State-Of-The-Art Imaging of Pancreatic Neuroendocrine Tumors

[Eric P. Tamm, M.D.](#), [Priya Bhosale, M.D.](#), [Jeffrey H. Lee, M.D.](#), and [Eric Rohren, M.D., Ph.D.](#)



PNET liver metastases (white arrowheads) on multiphase CT are classically hyperdense to background on early arterial phases

Pancreatic neuroendocrine tumours: hypoenhancement on arterial phase computed tomography predicts biological aggressiveness

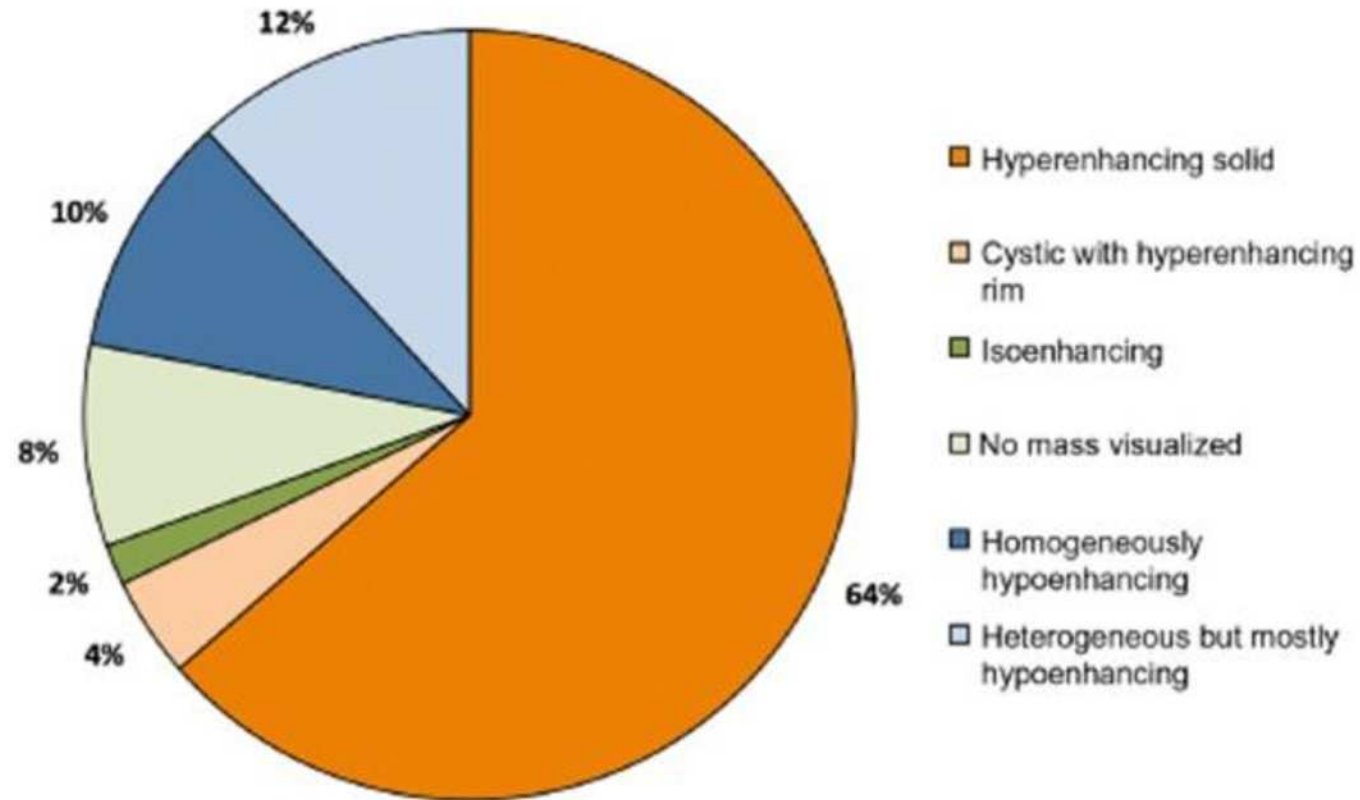
[David J Worhunsky](#),¹ [Geoffrey W Krampitz](#),¹ [Peter D Poulos](#),² [Brendan C Visser](#),¹ [Pamela L Kunz](#),³
[George A Fisher](#),³ [Jeffrey A Norton](#),¹ and [George A Poultsides](#)¹

118 operated patients

22% of hypoenhanced tumors:

- larger diameter
- G2-3: 76% vs. 30% for hyperenhanced tumors
- more frequent N+ et M+ ($p < .001$)

Worst prognostic with 5 y survival: 54% vs 93%



Hüpvaskulaarne pankrease NET

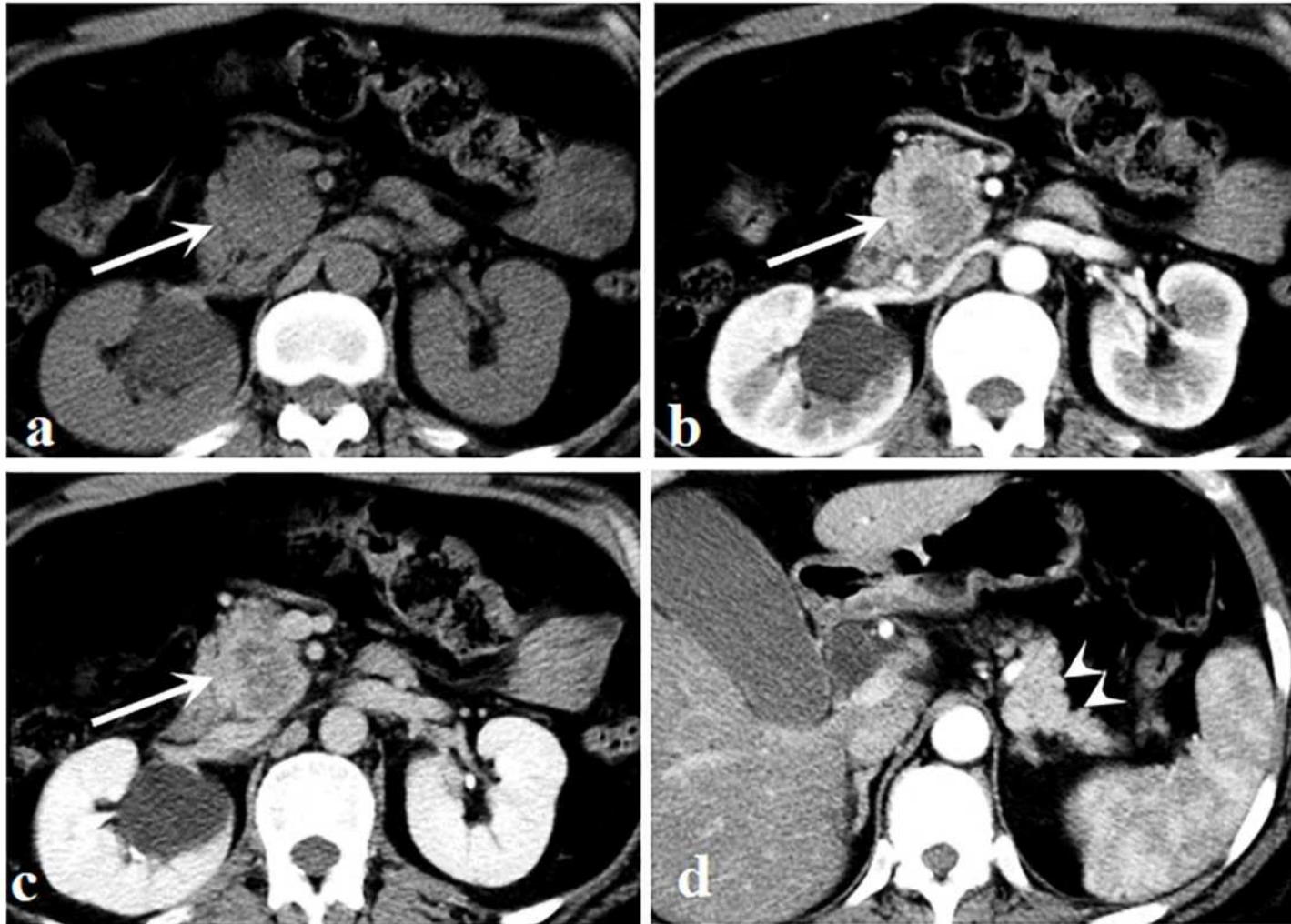


Fig 2. A 51-year-old woman with pancreatic neuroendocrine carcinoma. (a) Unenhanced image shows an isodense mass (arrow) located in the head of the pancreas. (b, c) Arterial (b) and portal venous (c) phase images show a well circumscribed mass (arrows) with a hypovascular enhancement pattern. (d) There was neither upstream pancreatic parenchymal atrophy nor pancreatic duct dilatation (arrowheads).

Differentiation of hypovascular pancreatic neuroendocrine tumors from pancreatic ductal adenocarcinoma using contrast-enhanced computed tomography

Shuai Ren, Xiao Chen, Zhonglan Wang, Rui Zhao, Jianhua Wang, Wenjing Cui, Zhongqiu Wang 

Published: February 1, 2019 • <https://doi.org/10.1371/journal.pone.0211566>

CT findings	hypo-PNETs (n = 18)	PDAC (n = 39)	P value	Correlation coefficient
Location			0.278 ^b	0.141
Head	9 (50)	22 (56.4)		
Body	3 (16.7)	11 (28.2)		
Tail	6 (33.3)	6 (15.4)		
Margin			0.016 ^b	0.320
Well-defined	10 (55.6)	9 (23.1)		
Ill-defined	8 (44.4)	30 (76.9)		
Calcification	1 (5.6)	3 (7.7)	1.0 ^b	0.039
Pancreatic duct dilatation	2(11.1)	23 (59)	0.002 ^b	0.448
Bile duct dilatation	2 (11.1)	14 (35.9)	0.106 ^b	0.256
Pancreatic Atrophy	4 (22.2)	20 (51.3)	0.076 ^b	0.274
Local invasion or Metastases	7 (38.9)	31 (79.5)	0.003 ^b	0.400
Size (cm)	4.3±1.6	3.8±1.3	0.20 ^a	0.242
Tumor contrast enhancement (HU)				
Arterial phase	59.8±8.7	44.2±9.2	<0.001 ^a	0.630
Portal venous phase	69.0±8.9	60.0±10.4	0.003 ^a	0.393
Delayed phase	66.6±10.6	60.6±10.5	0.083 ^a	0.261
Tumor-to-pancreas enhancement ratio				
Arterial phase	0.66±0.14	0.51±0.10	<0.001 ^a	0.536
Portal venous phase	0.71±0.15	0.61±0.12	0.010 ^a	0.338
Delayed phase	0.79±0.11	0.73±0.14	0.174 ^a	0.206

^a Calculated with a t-test

^b Calculated with a Fisher's exact test or an χ^2 test

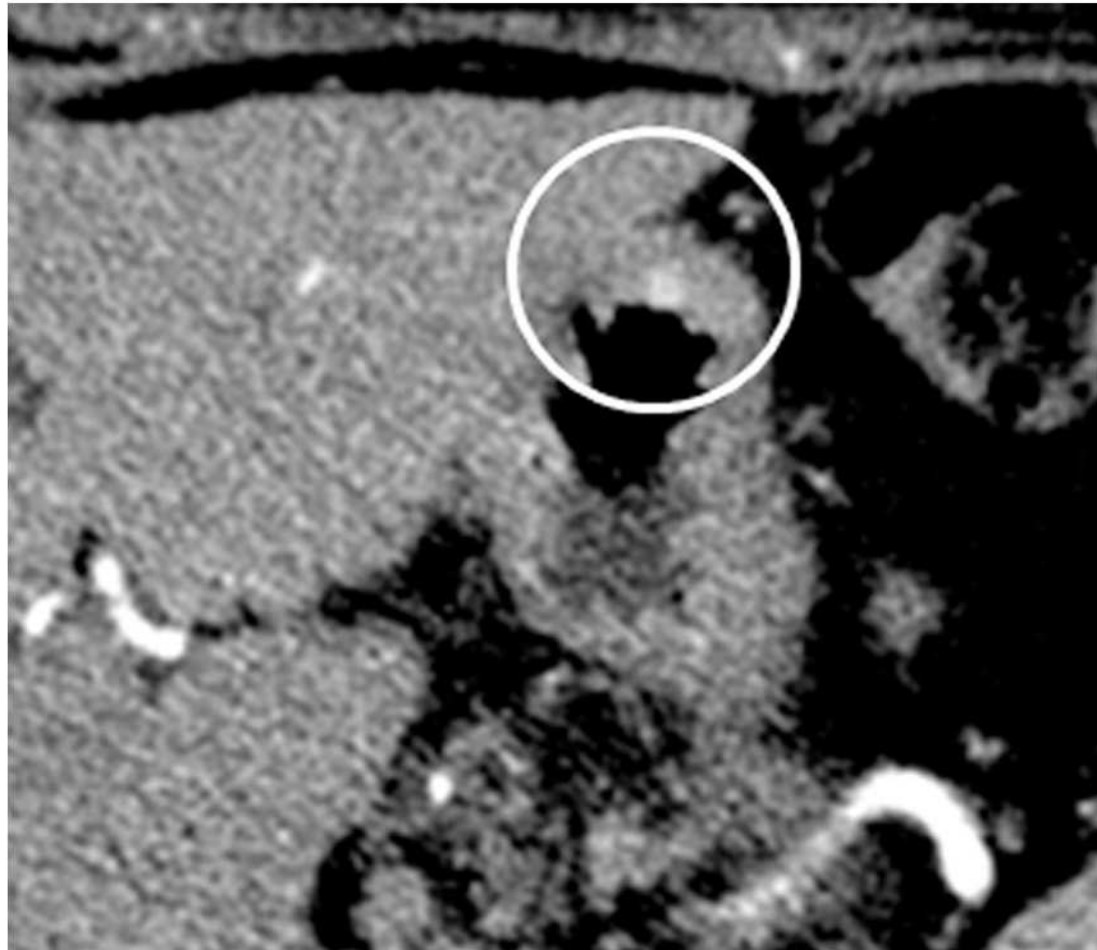
CT findings	AUC	Sensitivity (%)	Specificity (%)	Odds ratio	Confidence interval (95%)
Tumor margin	0.607	44.4	76.9	0.375	0.114–1.234
Pancreatic duct dilatation	0.739	59	88.9	11.5	2.316–57.101
Local invasion or Metastases	0.703	79.5	61.1	6.089	1.788–20.741
Tumor contrast enhancement (arterial)	0.888	88.9	77	0.839	0.765–0.921
Tumor contrast enhancement (portal)	0.748	94.4	54.3	0.917	0.863–0.975
Tumor-to-pancreas enhancement ratio (arterial)	0.812	83.3	61.6	0.034	0–4.444
Tumor-to-pancreas enhancement ratio (portal)	0.693	83.3	53.9	0.003	0–0.357

<https://doi.org/10.1371/journal.pone.0211566.t003>

Table 3. The receiver operating characteristic analysis of CT findings in differentiating hypovascular pancreatic neuroendocrine tumors (hypo-PNETs) from pancreatic ductal adenocarcinoma (PDAC).

Multimodality Imaging Findings in Carcinoid Tumors: A Head-to-Toe Spectrum

Ameya Jagdish Baxi [✉](#), Kedar Chintapalli, Amol Katkar, Carlos S. Restrepo, Sonia L. Betancourt, Abhijit Sunnapwar



Axial contrast-enhanced multidetector CT image of the abdomen demonstrates a small enhancing nodule (circle) in the gastric wall

Gastrointestinal (74)

- Appendix (18.9)
- Ileum (15.4)
- Rectum (11.4)
- Cecum (4.2)
- Stomach (3.2)
- Duodenum (2.0)
- Jejunum (1.9)
- Rectosigmoid (1.2)
- Ascending colon (1.0)
- Other sites* (<1)

Respiratory (25)

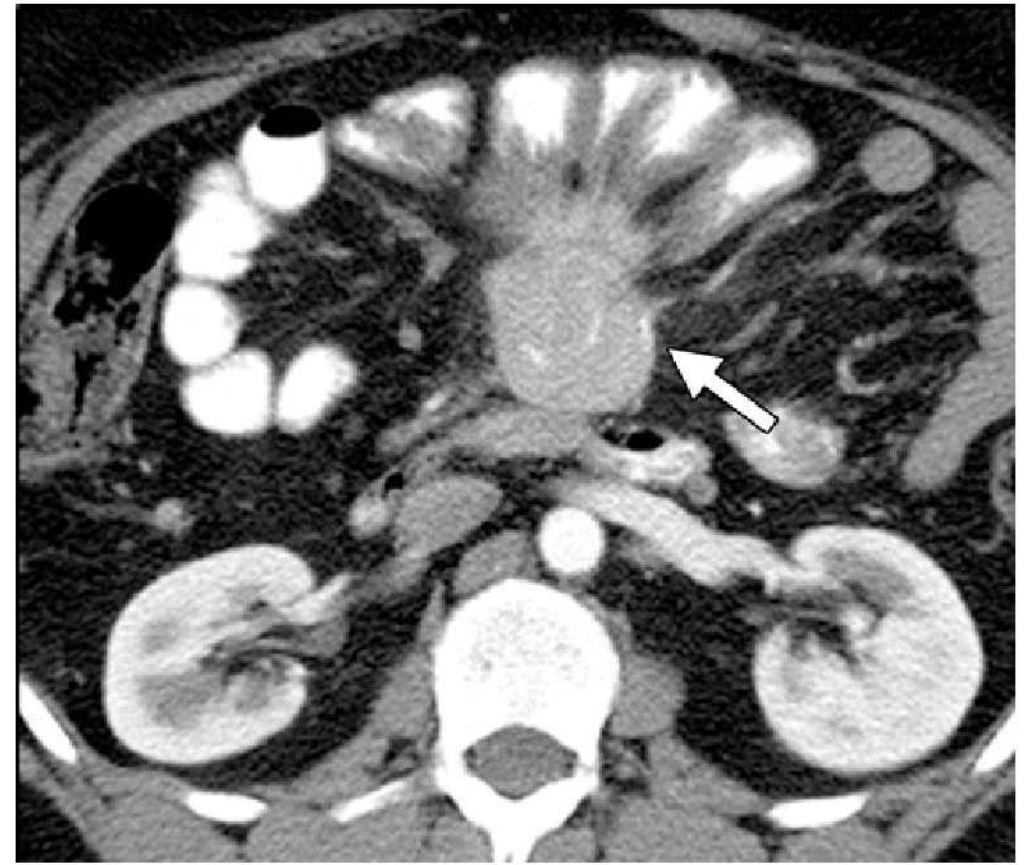
- Trachea
- Bronchi
- Lung

Reproductive (0.56)

- Ovary
- Cervix
- Uterine corpus
- Testes

Unspecified (0.6)

- Thymus
- Head and neck
- Breast



(b) Axial multidetector CT image of the abdomen demonstrates a partially calcified soft-tissue mass (arrow) in the mesentery with adjacent desmoplastic reaction and spoke-wheel or sunburst arrangement of mesenteric vessels.

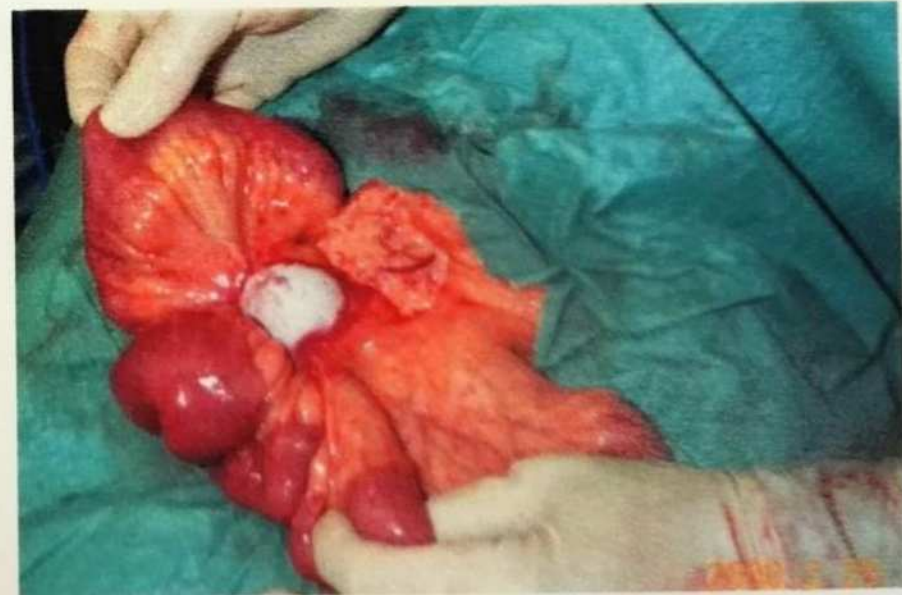
85% peensoole NET-dest distaalses iileiumis

Neuroendocrine neoplasms of the small intestine

Clinical manifestations

Related to primary tumor

- None
- Abdominal discomfort (for years)
- Diarrhoea
due to partial bowel obstruction or ischemia
- Small bowel obstruction
- Vascular encasement
Intestinal ischemia or infarction
- Malnutrition
- Gastrointestinal bleeding (rarely)
- Intussusception
- Mesenteric fibrosis
- Abdominal mass

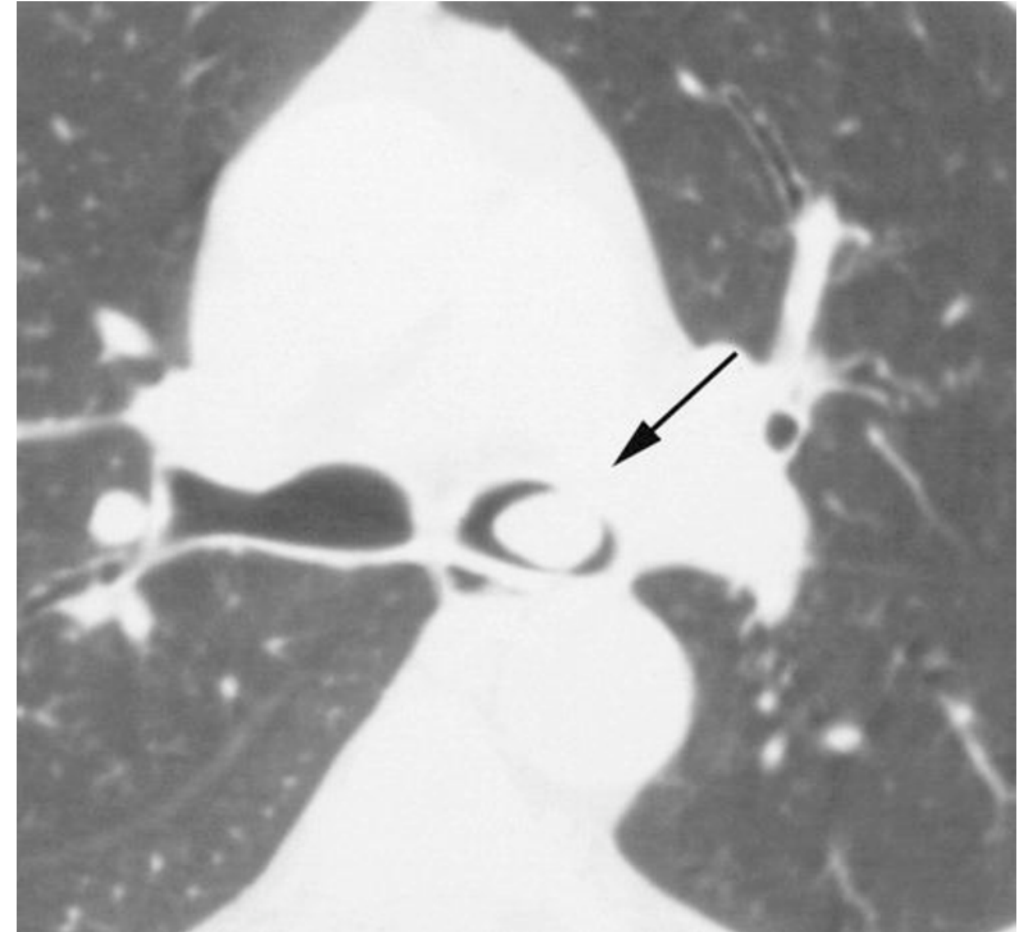


Bronchial Carcinoid Tumors of the Thorax: Spectrum of Radiologic Findings

Mi-Young Jeung, Bernard Gasser, Afshin Gangi, Dominique Charneau, Xavier Ducroq, Romain Kessler, Elisabeth Quoix, Catherine Roy

- Tsentraalsed ja perifeersed
- Endobronhiaalne tuumor - obstruktsioon

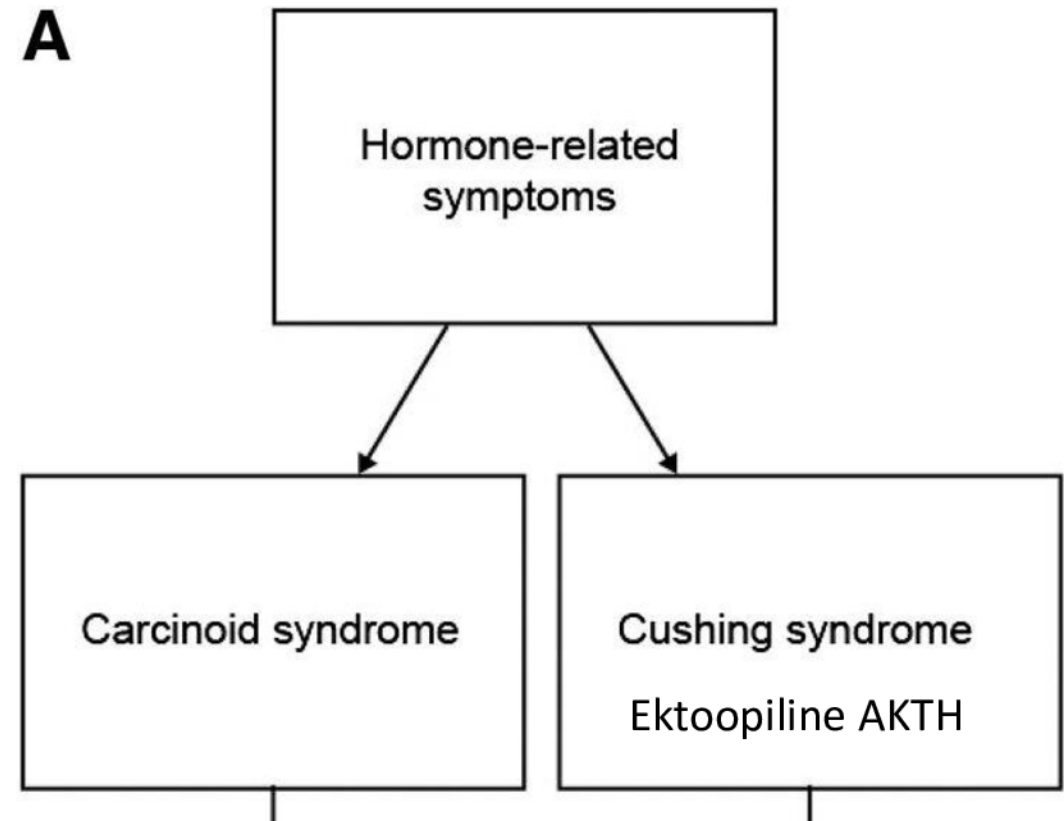
RadioGraphics



b) CT scan (lung windowing) shows a well-circumscribed, ovoid, completely endoluminal nodule (arrow).

Bronhopulmonaarsed NET-id

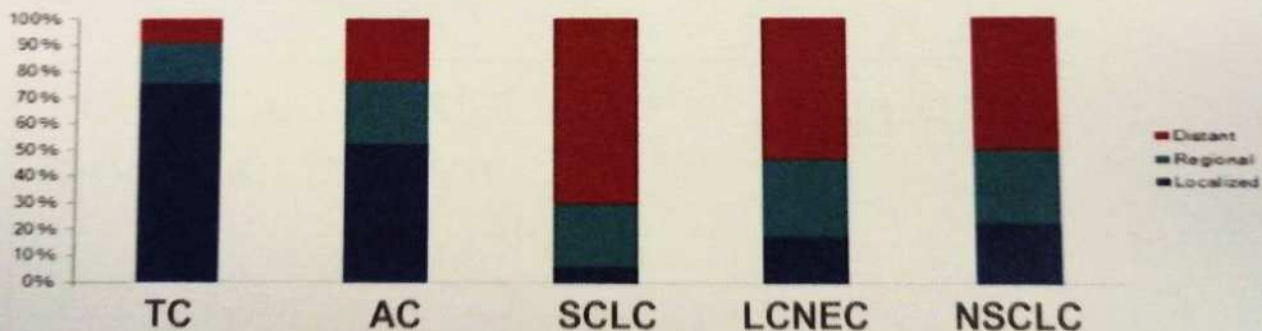
- Tüüpiline kartsionid, *TC*
- Atüüpiline kartsinoid, *AC*
- Suur-rakk neuroendokriinne kasvaja, *LCNEC*
- Väike-rakk kopsuvähk, *SCLC*



Stage, histology, and prognosis

SEER 2000-2010

Survival (months)	Localized	Regional	Distant
TC	>120	>120	42
AC	>120	70	12
LCNEC	30	13	3
SCLC	16	12	5



For TC, surgical resection provides excellent outcomes, with 5- and 10-year survival rates of ~90% and ~80%, respectively, and very low recurrence rates (3%–5%).

ACs are notably more aggressive than TCs, with a higher frequency of regional lymph node involvement (50%–60% vs. 10%–15%) and distant metastasis (~20% vs. 2%–5%) and worse survival outcomes at 5 years (56%–79% vs. 87%–96%) and 10 years (35%–56% vs. 82%–87%)

50,000 meters

40,000 meters

30,000 meters

20,000 meters

10,000 meters

Theoretical Tsar Bomba

Tsar Bomba

Red Bull Stratos Height



Castle Bravo

B83 Bomb

Average commercial airliner altitude



Hiroshima

Nagasaki

Mt. Everest

NM to image NEN: tracers targeting

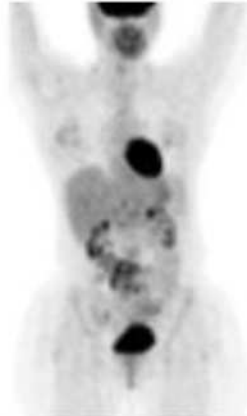
PET/CT

METABOLISM

18F-DOPA



18F-FDG



SOMATOSTATIN RECEPTORS

AGONISTS (SA)
68Ga-DOTA-TATE
68Ga-DOTA-NOC
68Ga-DOTA-TOC



64Cu-DOTA-TATE

THERANOSTIC

¹⁷⁷Lu-DOTA-TATE

SOMATOSTATIN RECEPTORS

SCINTIGRAPHY

SPECT/CT



¹¹¹In-OCT

^{99m}Tc-TOC

Molecular imaging for neuroendocrine tumours

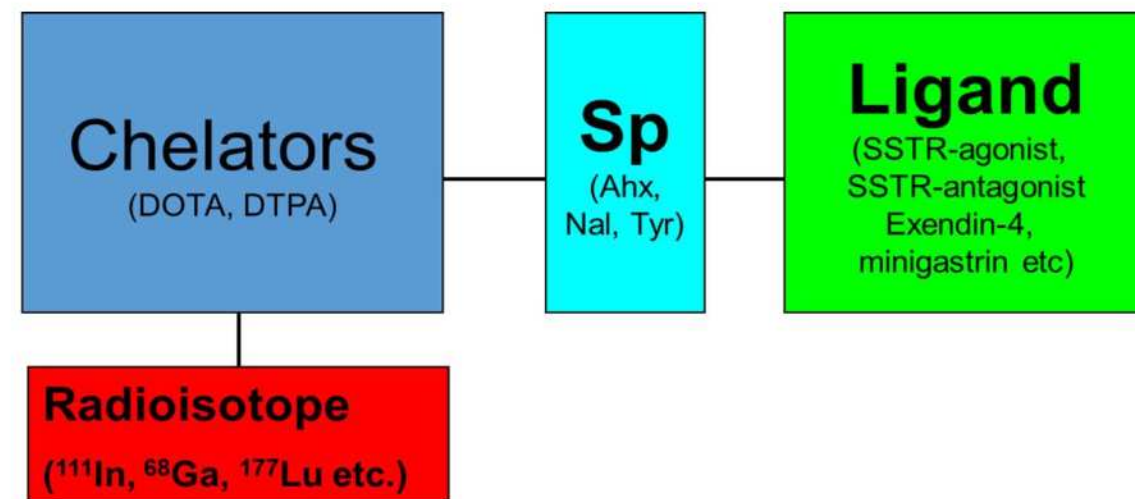
DOI: <https://doi.org/10.4414/sm.w.2019.20017>

Publication Date: 10.03.2019

Swiss Med Wkly. 2019;149:w20017

Swiss Medical
Weekly

- 5 somastatiin retseptorie alatüübi
- SSR 2 –tihedalt ja homogeenselt ekspresseeritud NET tuumorite rakkude pinnal 80-90% juhtudest.
- Erandid: insulinoomid ja kilpnäärme medullaarne vähk
- muud retseptorud GLP-1 ja CCK-2
- SSR enam G1 ja G2 tuumoritel, Ki67 1-20%



G1 NET

G2 NET

G3 NET

G3 NEC

Differentiation

.....**well differentiated**.....

Poorly differentiated

Evolution

slow

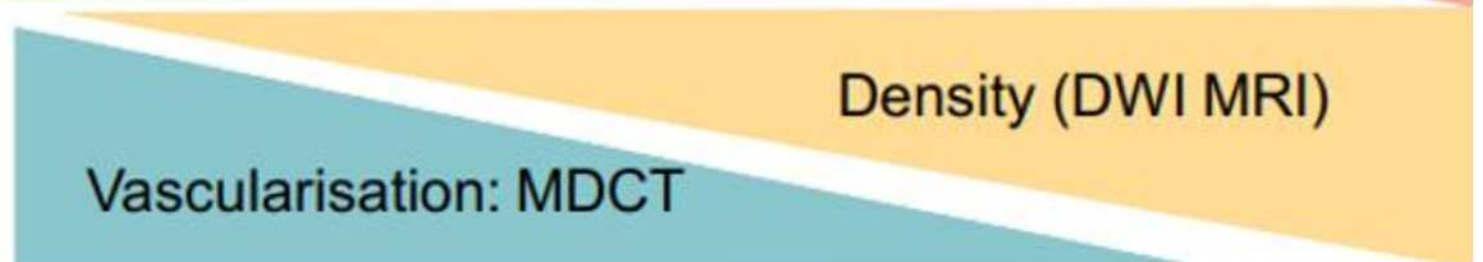


fast/bad pronostic

Nuclear Imaging



Functional Imaging MDCT/MRI

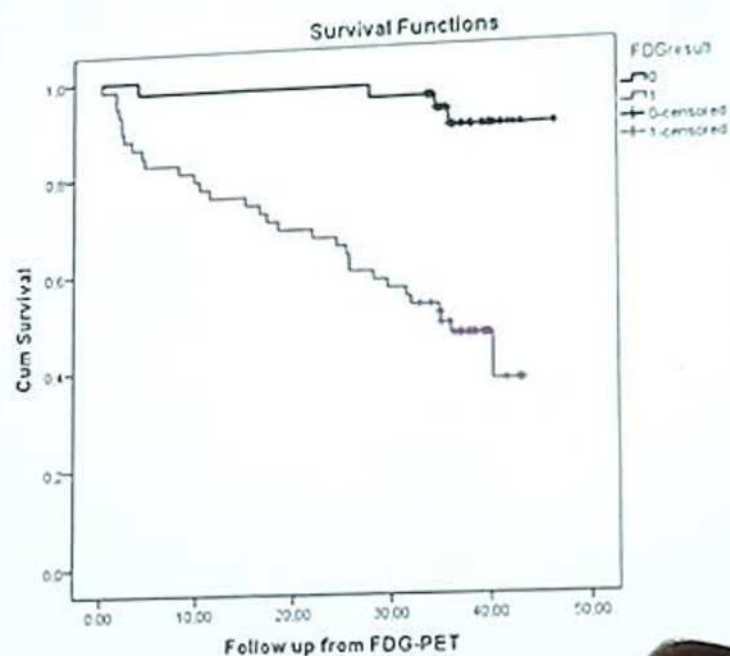


FDG-PET in neuroendocrine tumors

Clinical
Cancer
Research

Imaging, Diagnosis, Prognosis

^{18}F -Fluorodeoxyglucose Positron Emission Tomography
Predicts Survival of Patients with Neuroendocrine Tumors



Somatostatin Receptor Imaging with ^{68}Ga DOTATATE PET/CT: Clinical Utility, Normal Patterns, Pearls, and Pitfalls in Interpretation



^{111}In -DTPA-octreotide SPECT/CT:

^{111}In — DTPA — Octreotide

SSTR subtype 3-5

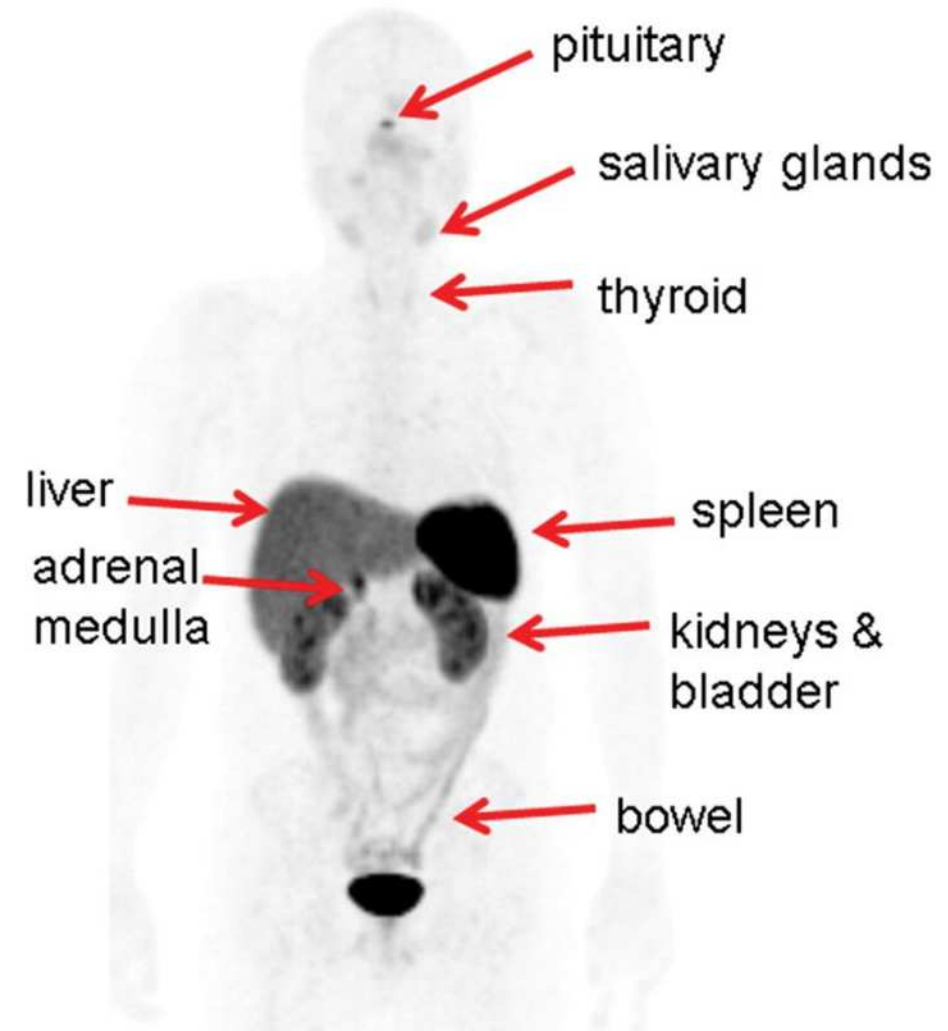
DOTATATE (GaTate) PET/CT:

^{68}Ga — DOTA — Octreotate

SSTR subtype 2

Somatostatiin retseptorite e. SSR kuvamine

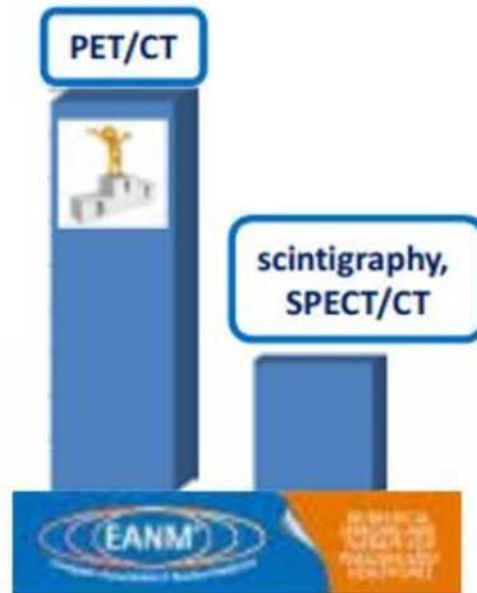
- Teadmata algkolde otsimine
- Staadiumi määramine
- ^{177}Lu -peptiid ravi planeerimine



NM to image NEN: procedures..

Guideline for PET/CT imaging of neuroendocrine neoplasms with ^{68}Ga -DOTA-conjugated somatostatin receptor targeting peptides and ^{18}F -DOPA

Murat Fani Bozkurt¹ · Irene Virgolini² · Sona Balogova^{3,4} · Mohsen Beheshti^{5,6} · Domenico Rubello⁷ · Clemens Decristoforo² · Valentina Ambrosini⁸ · Andreas Kjaer⁹ · Roberto Delgado-Bolton¹⁰ · Jolanta Kunikowska¹¹ · Wim J. G. Oyen¹² · Arturo Chiti¹³ · Francesco Giammarile¹⁴ · Stefano Fanti⁸



PET/CT whenever possible

^{68}Ga -DOTATATE PET/CT, $^{99\text{m}}\text{Tc}$ -HYNIC-Octreotide SPECT/CT, and Whole-Body MR Imaging in Detection of Neuroendocrine Tumors: A Prospective Trial

Neuro
endocrinology

Download Fulltext PDF

Free Access

At the Cutting Edge

The Status of Neuroendocrine Tumor Imaging: From Darkness to Light?

ESMIT

European School of Multimodality Imaging and Therapy



The Status of Neuroendocrine Tumor Imaging: From Darkness to Light?

Bodei L.^a · Sundin A.^b · Kidd M.^c · Prasad V.^d · Modlin I.M.^c

Fig. 2

Methods for the identification of primary and metastatic gastroenteropancreatic NETs. Data are pooled from 52 studies and are mean (95% confidence interval). Data for specificity and sensitivity are not comparable across studies. S = Calculated sensitivity.

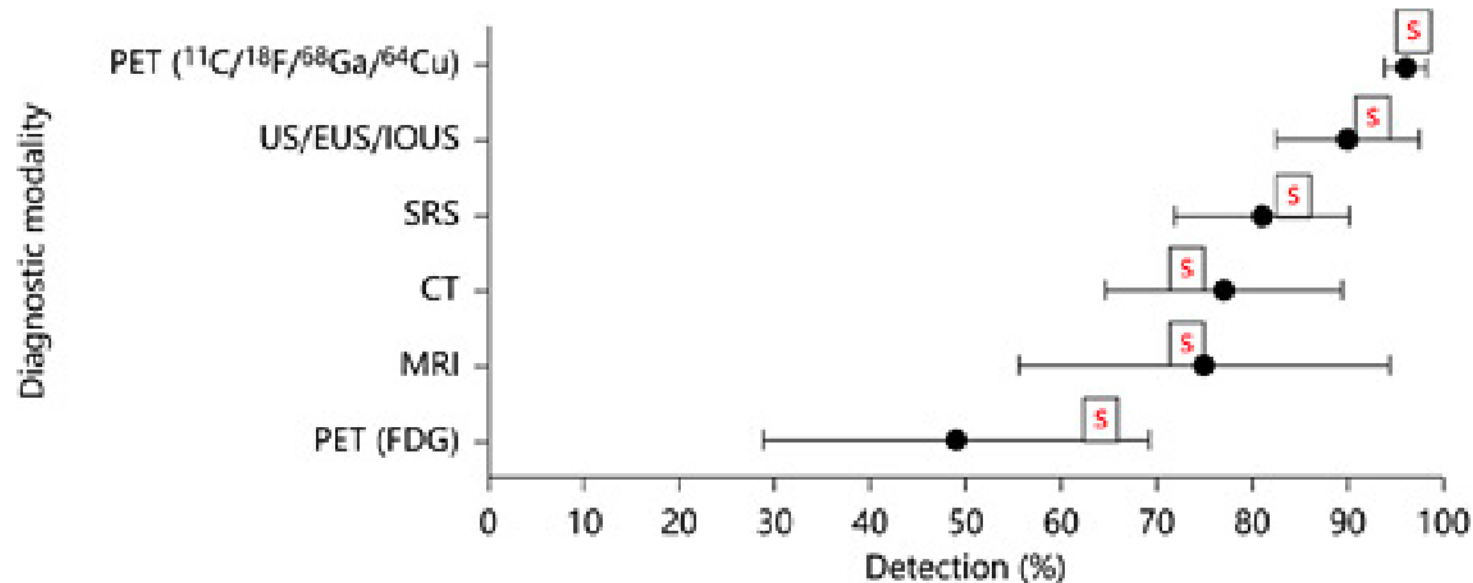


Table 3 Proposed diagnostic strategy based on the NEN type

Type of NEN	Place in diagnostic strategy (I-II-III)*		
	⁶⁸ Ga-somatostatin analogue	¹⁸ F-DOPA	¹⁸ F-FDG
Medullary thyroid cancer	III mainly when treatment with SST analogues is an option	In patients with high serum calcitonin levels: I In patients with high serum CEA levels II	In patients with high serum calcitonin levels II In patients with high serum CEA levels I
Foregut NET	I	Not indicated	I
Midgut NET	I	I	II
Hindgut-NET	II	II	I
Pheochromocytoma	II/III	With SDHD mutation I With SDHB mutation II-	With SDHD mutation II With SDHB mutation I
Paraganglioma	Head and neck	Head and neck	Head and neck
	I	II	III
	Abdomen/pelvis	Abdomen/pelvis	Abdomen/pelvis
	II	I	III
CUP NET	If suspected primary foregut I	If suspected primary midgut I	To localise the primary tumour and eventual non-NET malignancy I
Neuroblastoma		I	Older age, advanced stages or MYCN amplification I
Hyperinsulinism in infants and in children		II	

CUP: carcinoma of unknown primary

*I: The first choice proposed

II: The second choice proposed

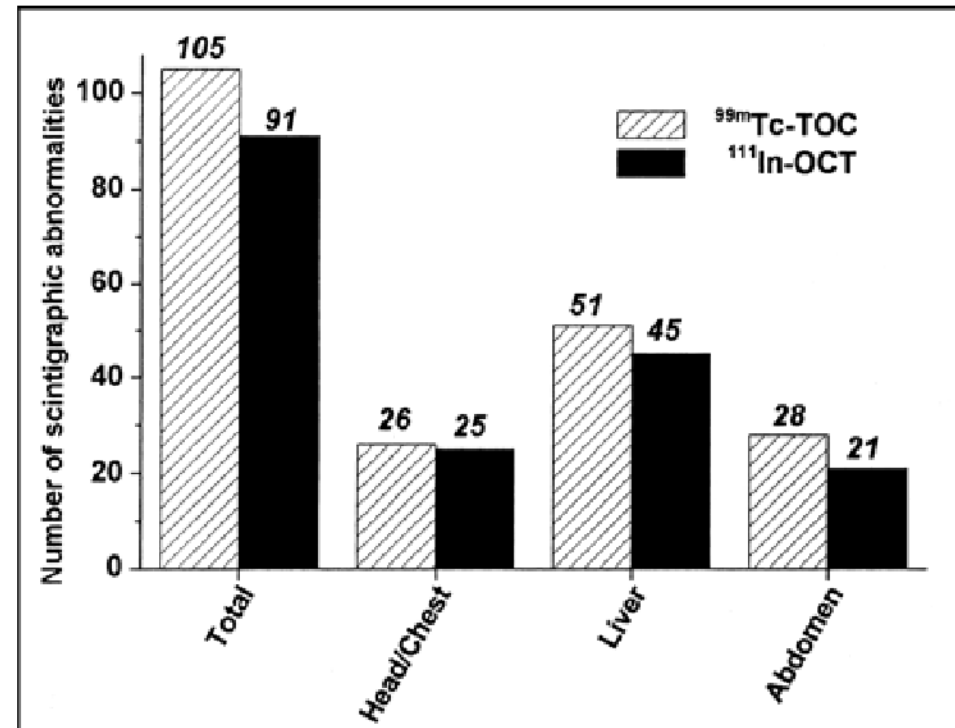
III: The third choice proposed

Somatostatiin retseptorite stsintigraafia ja SPET/KT

- ^{111}In -OCT – OctreoScan (Mallinckrodt Medical)
- $^{99\text{m}}\text{Tc}$ -TOC - Tektrotyd (Polatom)

An Inpatient Comparison of $^{99\text{m}}\text{Tc}$ -EDDA/HYNIC-TOC with ^{111}In -DTPA-Octreotide for Diagnosis of Somatostatin Receptor-Expressing Tumors

Michael Gabriel, MD¹, Clemens Decristoforo, PhD¹, Eveline Donnemiller, MD¹,



SSR agonistid PET/KT DOTA-peptiidid

- Diagnostikum:

^{68}Ga -DOTATATE, -DOTATOC, -DOTANOC

^{64}Cu - DOTATATE

- Terapeutikum:

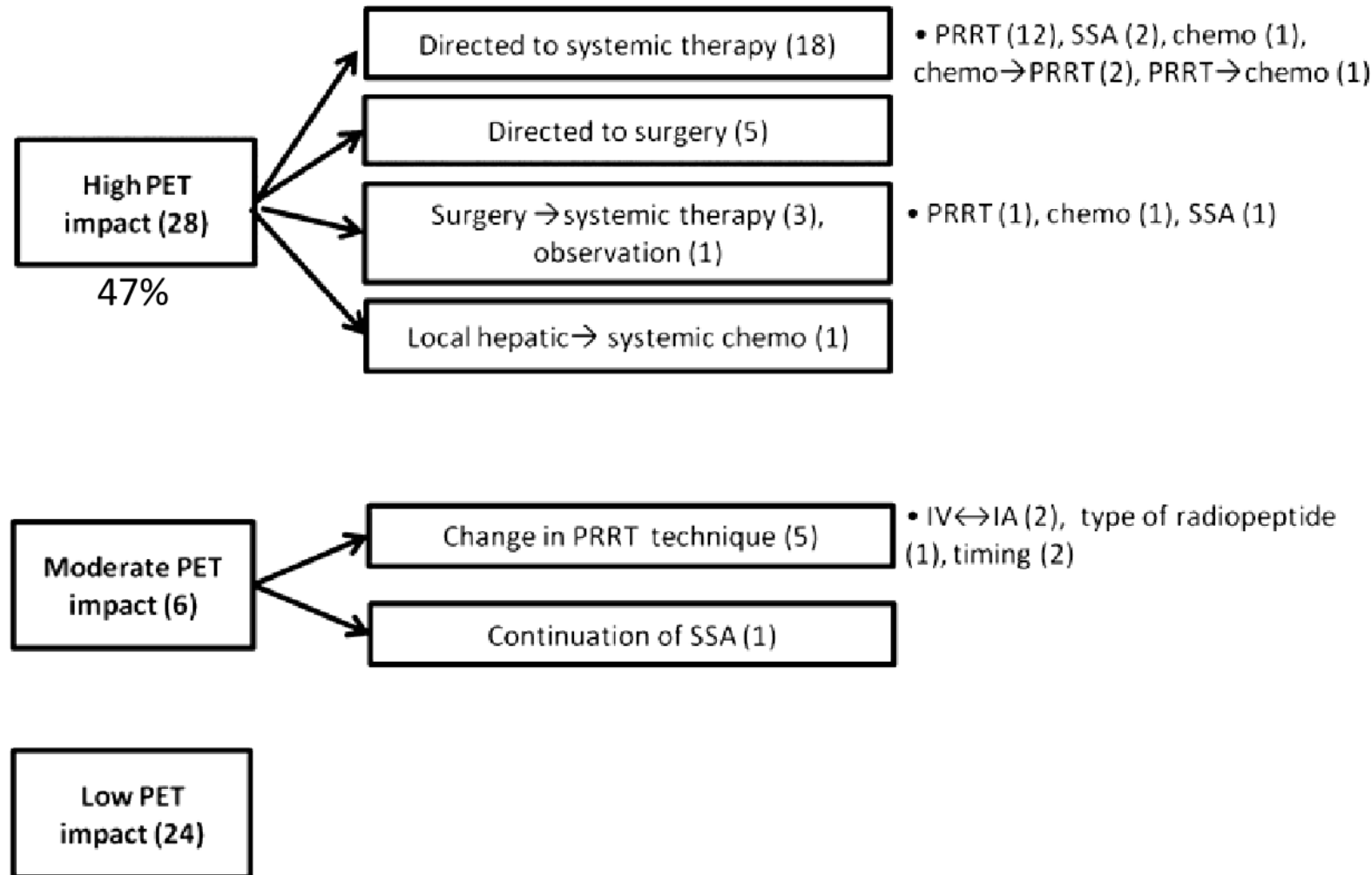
^{177}Lu -DOTATATE - TERANOSTIKA



High management impact of Ga-68 DOTATATE (GaTate) PET/CT for imaging neuroendocrine and other somatostatin expressing tumours



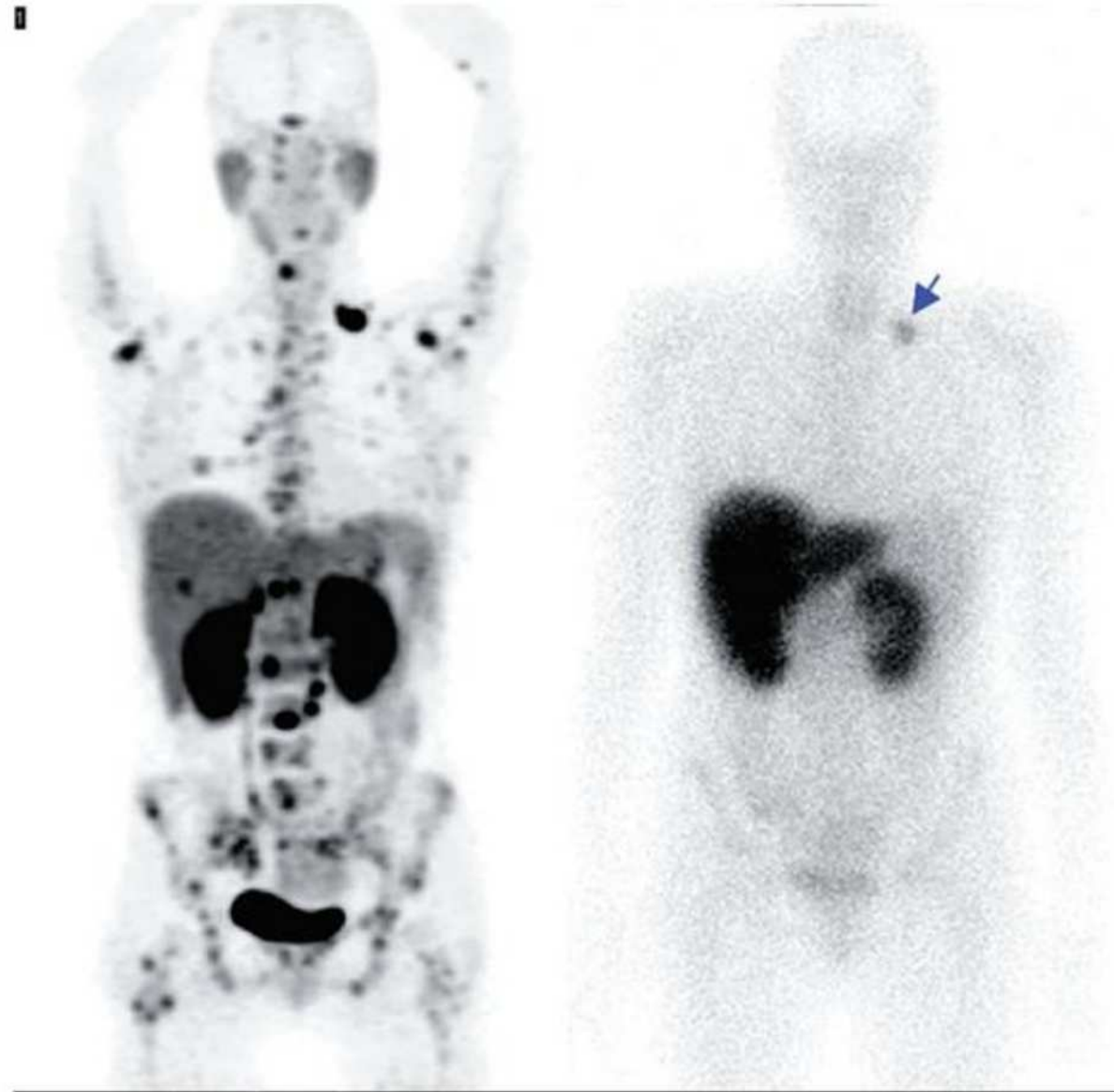
Michael S Hofman , Grace Kong, Oliver C Neels, Peter Eu, Emily Hong, Rodney J Hicks



In patients who underwent ¹¹¹In-octreotide imaging in the preceding 3, 3–6 or >6 months, there was a high management impact in 71, 40 and 50%; the greater impact in patients imaged within a shorter time window suggests that results have not been confounded by disease progression between scans.

Fig. 3. Management impact. High impact denotes an inter-modality change and moderate impact denotes an intra-modality change. Chemo, chemotherapy; IA, intra-arterial; IV, intravenous; PET, positron emission tomography; PRRT, peptide receptor radionuclide therapy; SSA, long-acting somatostatin analogue.

Fig. 4. Middle age woman with long-standing history of 'chronic pancreatitis'. At second operation found to have sub-centimetre hepatic metastasis with histology demonstrating well-differentiated neuroendocrine tumour. Triple phase CT scan demonstrated no abnormality apart from multiple sclerotic bone lesions considered to be benign bony islands (osteopoikilyosis) with prior 'negative' bone biopsy. ^{111}In -octreotide scan (top right) anterior planar and single photon emission tomography/CT (not shown) demonstrated a solitary left supraclavicular nodal abnormality (blue arrow). GaTate positron emission tomography (PET)/CT scan (top left: anterior maximum image projection, bottom: selected axial PET/CT fusion slices) performed 1 week later demonstrated a pancreatic primary and sub-centimetre liver metastasis (red arrows), and widespread nodal and osseous metastases. The patient subsequently underwent radionuclide therapy with ^{177}Lu -octreotate.



⁶⁸Ga-DOTATATE PET/CT, ^{99m}Tc-HYNIC-Octreotide SPECT/CT, and Whole-Body MR Imaging in Detection of Neuroendocrine Tumors: A Prospective Trial

Elba Cristina Sá de Camargo Etchebehere¹, Allan de Oliveira Santos¹, Brenda Gumz², Andreia Vicente¹, Paulo G Gustavo Corradi³, Wilson André Ichiki¹, José Geraldo de Almeida Filho¹, Saulo Cantoni³, Edwaldo Eduardo C and Frederico Prego Costa²

Results: McNemar testing was applied to evaluate the detectability of lesions using ⁶⁸Ga-DOTATATE PET/CT in comparison to SSRS SPECT/CT and WB DWI: a significant difference in detectability was noted for **pancreas, gastrointestinal, and bones.**

Two **unknown primary lesions** were identified solely by ⁶⁸Ga-DOTATATE PET/CT. ⁶⁸Ga-DOTATATE PET/CT, SSRS SPECT/CT, and WB DWI demonstrated, respectively, sensitivities of 0.96, 0.60, and 0.72; specificities of 0.97, 0.99, and 1.00;

TABLE 1
Lesion Detection Capability of SSRS SPECT/CT, ⁶⁸Ga PET/CT, and WB DWI

Variable	N/P	P value	
		⁶⁸ Ga-DOTATATE PET/CT vs. SSRS SPECT/CT	⁶⁸ Ga-DOTATATE PET/CT vs. WB DWI
All solid organs	N P	0.0253	0.0833
Lungs and pleura	N P	1.0000	0.1573
Liver	N P	0.1573	0.3173
Pancreas	N P	0.0455	0.0455
Gastrointestinal tract	N P	0.0455	0.0455
All LNs	N P	0.5637	1.0000
Cervical LNs	N P	1.0000	1.0000
Thoracic LNs	N P	0.5637	0.0833
Abdomen and pelvic LNs	N P	0.3137	0.3173
All skeletal system	N P	0.0082	0.0082
Bones of spine and pelvis	N P	0.0143	0.0455
Thoracic bones	N P	0.0143	0.0143
Bones of limbs	N P	0.0253	0.0455
Skull and skull base	N P	0.0455	0.0455

LNs = lymph nodes; N = negative; P = positive.

Comparison of diagnostic accuracy of ^{111}In -pentetreotide SPECT and ^{68}Ga -DOTATOC PET/CT: A lesion-by-lesion analysis in patients with metastatic neuroendocrine tumours

S. Van Binnebeek¹ · B. Vanbilloen¹ · K. Baete¹ · C. Terwinghe¹ · M. Koole¹ · F. M. Mottaghy^{2,3} · P. M. Clement⁴ · L. Mortelmans¹ · K. Bogaerts⁵ · K. Haustermans⁶ · K. Nackaerts⁷ · E. Van Cutsem⁸ · C. Verslype⁸ · A. Verbruggen⁹ · C. M. Deroose^{1,10}

Table 3 Lesion-based organ-by-organ comparison of ^{68}Ga -DOTATOC PET_{FOVSPECT} and ^{111}In -pentetreotide single-photon emission computed tomography (SPECT) for the liver, the lymph nodes

(LN), the bone and other regions (not bone, lymph nodes or liver). The total number of lesions as well as the incremental lesions (ILs) are given; we also added the number of patients in whom ILs were seen

Organ	No. of lesions PET _{FOVSPECT}	No. of lesions SPECT _{total}	P-value	IL* _{PET}	IL* _{SPECT}	No. of patients with IL _{PET} (n=53)	No. of patients with IL _{SPECT} (n=53)
Liver	593	395	9.7×10^{-5}	199	1	35 (66 %)	1 (2 %)
LN	183	129	2.9×10^{-5}	54	0	14 (26 %)	0
Bone	249	86	5.5×10^{-2}	163	0	14 (26 %)	0
Other	73	50	2.1×10^{-2}	23	0	9 (17 %)	0
Total	1,098	660	1.7×10^{-5}	439	0	42 (79 %)	1 (2 %)

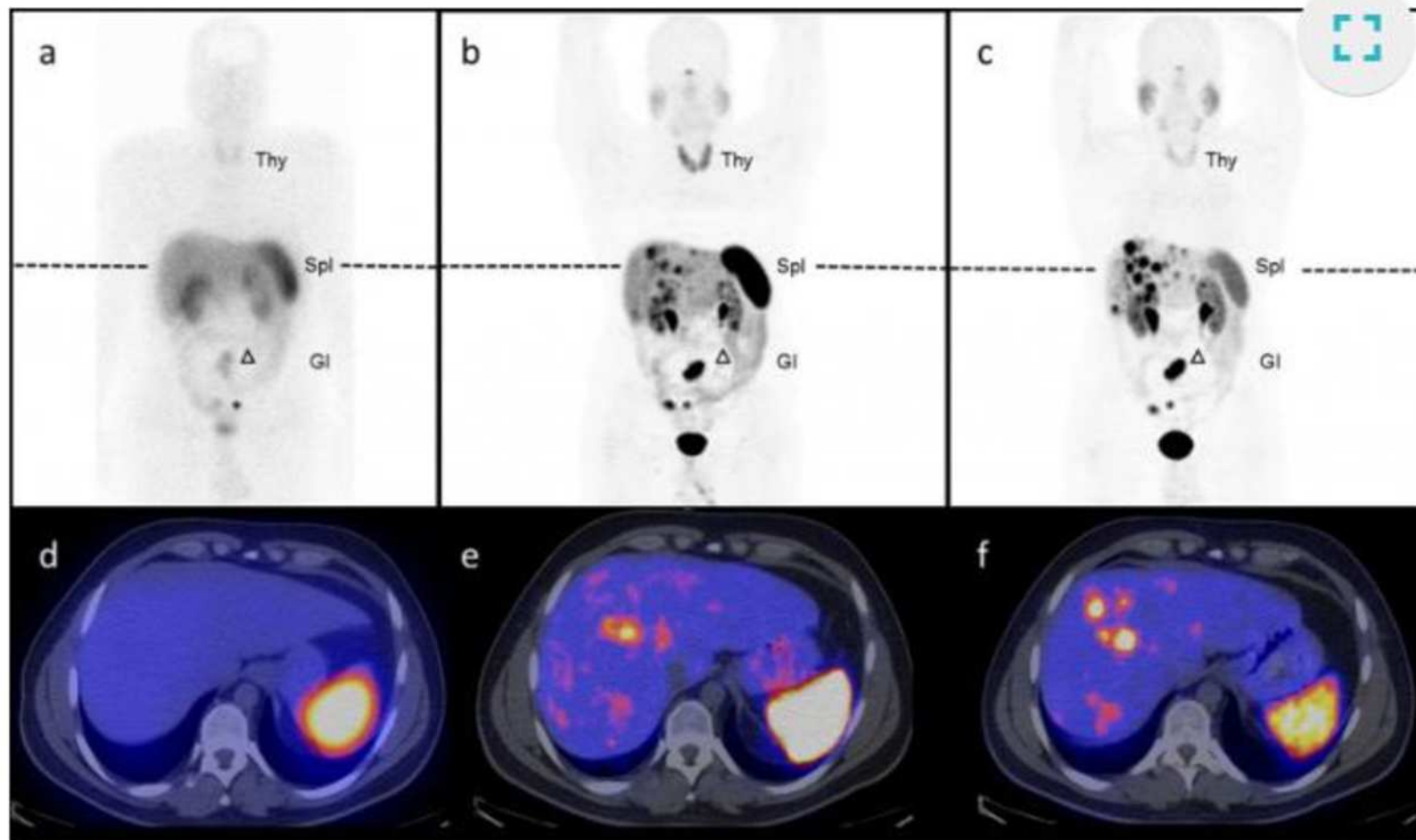
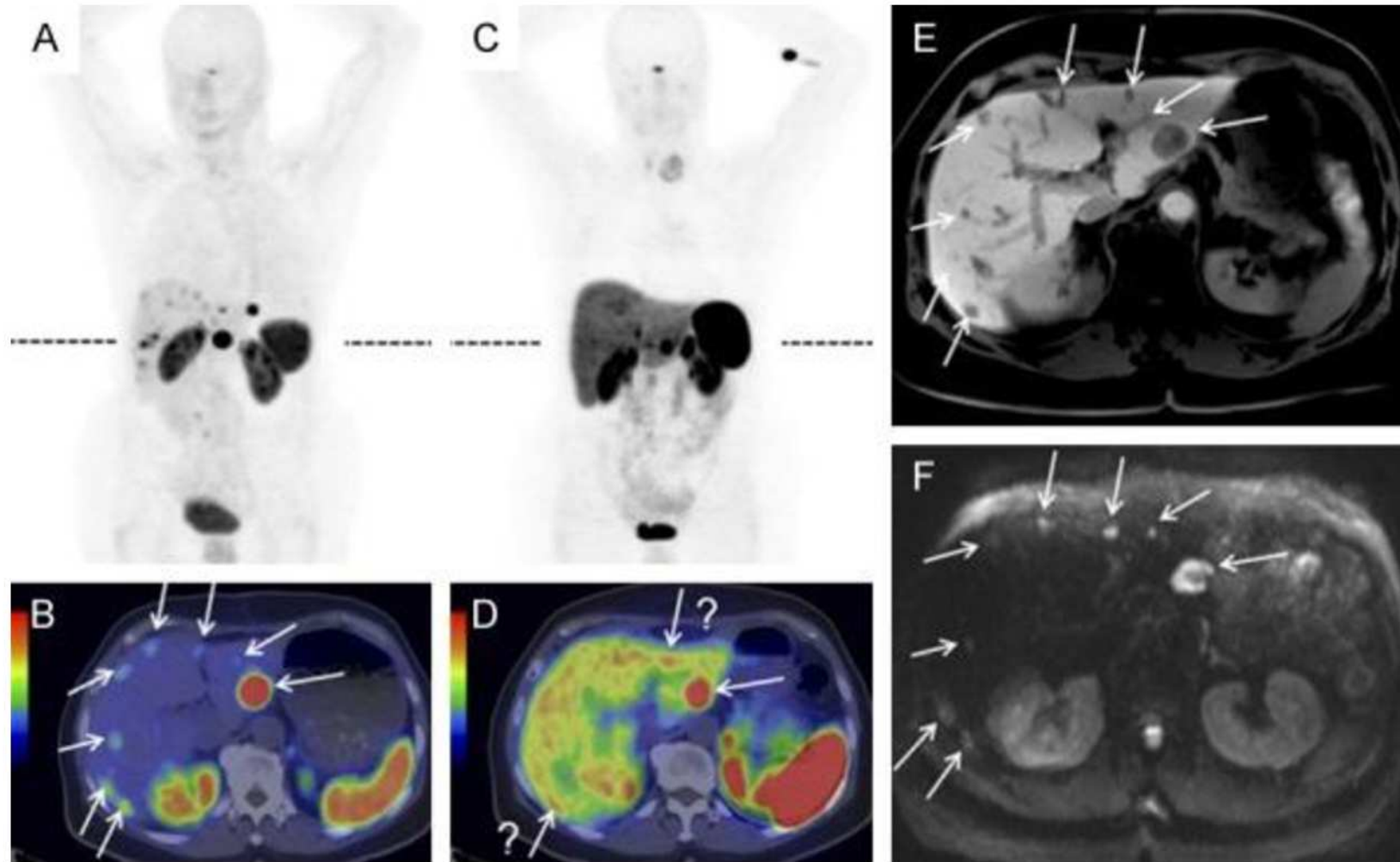


Figure 3

Somatostatin-receptor targeting using ^{111}In -DTPA-octreotide, ^{68}Ga -DOTA-octreotide and ^{68}Ga -DOTA-SSTR-antagonist. Head-to-head comparison of ^{111}In -DTPA-octreotide scintigraphy and SPECT/CT

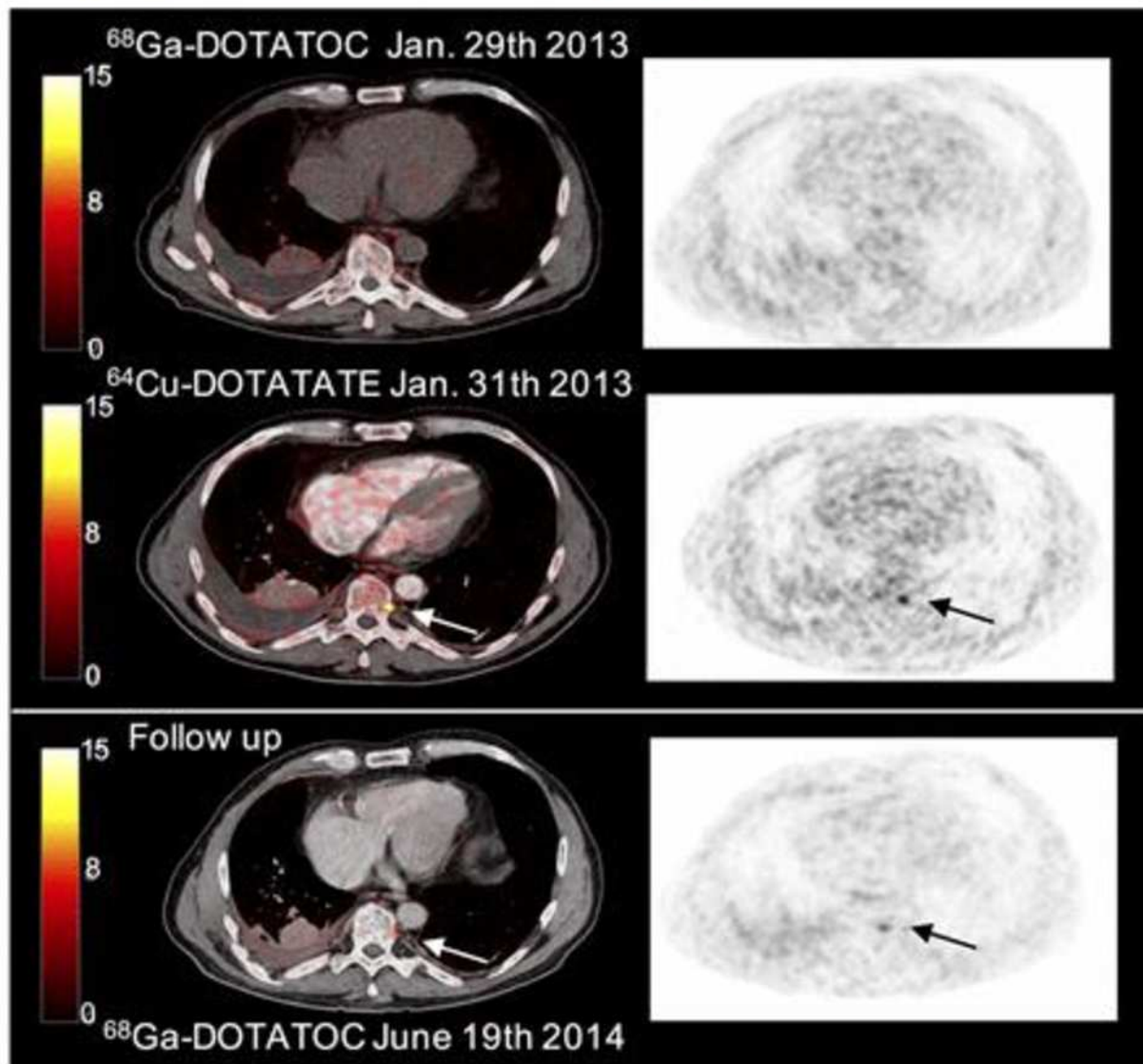
SSR antagonistid....



Maximal-intensity projections (A and C) and PET/CT (B and D) scans with ^{68}Ga -NODAGA-JR11 (A and B) and ^{68}Ga -DOTATOC of a patient with ileal NET and bilobar liver metastases.

Head-to-Head Comparison of ^{64}Cu -DOTATATE and ^{68}Ga -DOTATOC PET/CT: A Prospective Study of 59 Patients with Neuroendocrine Tumors

Camilla B. Johnbeck^{1,2}, Ulrich Knigge^{2,3}, Annika Loft^{1,2}, Anne K. Berthelsen^{1,2}



Editorial | Published: 07 August 2019

Al^{18}F -NOTA-octreotide and ^{18}F -SiFAlin-TATE: two 'new kids on the block' in somatostatin receptor imaging

J Nucl Med. 2015 Jul;56(7):1100-5. doi: 10.2967/jnumed.114.149583. Epub 2015 May 14.

In Vivo Evaluation of ^{18}F -SiFAlin-Modified TATE: A Potential Challenge for ^{68}Ga -DOTATATE, the Clinical Gold Standard for Somatostatin Receptor Imaging with PET.

Niedermoser S¹, Chin J², Wängler C³, Kostikov A², Bernard-Gauthier V⁴, Vogler N⁵, Soucy JP⁶, McEwan AJ⁷, Schirmacher R⁴, Wängler B¹.

...

^{64}Cu -DOTATATE: first-in-humans (n=14)

- Safe
- Favorable dosimetry of 6.3 mSv at dose of 200 MBq
- Dose reduction possible (150 MBq or lower)

Table 6. Absorbed doses in the most exposed organs and the effective doses of somatostatin receptor tracers.

Organ/dose	^{67}Ga -DOTANOC [81]	^{67}Ga -DOTATOC [82]	^{67}Ga -DOTATATE [83]	^{64}Cu -DOTATATE [83]	^{111}In -DTPAOC [86]	^{111}In -DOTATOC [86]
Kidneys (mGy/MBq)	0.09	0.22	0.09	0.14	0.47	0.50
Liver (mGy/MBq)	0.03	0.07	0.05	0.16	0.07	0.05
Spleen (mGy/MBq)	0.07	0.24	0.28	0.12	0.36	0.47
Bladder (mGy/MBq)	0.08	0.07	0.13	0.04	0.19	0.16
Effective dose (mSv/MBq)	0.02	0.02	0.03	0.03	0.05	0.05
Typical administered dose (MBq)	120-200	120-200	120-200	180-220	111-222	140-200
Radiation burden at a typical dose (mSv)	2.0-3.3	2.8-4.6	3.0-5.1	5.7-6.9	5.6-11.1	7.0-10.0

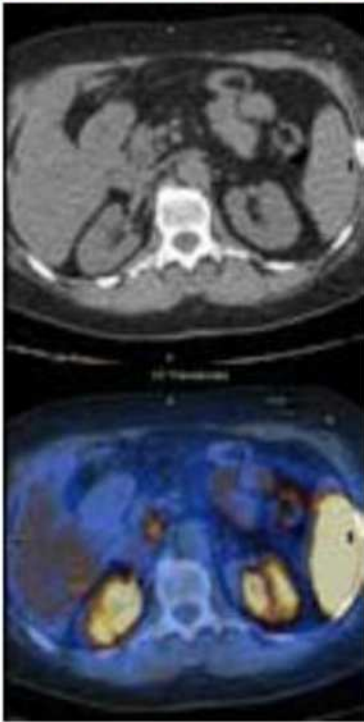
DOTANOC: DOTA-Tyr3-octreotide; DOTATATE: DOTA-Tyr3-octreotate; DOTATOC: DOTA-Tyr3-octreotide.

$^{99\text{m}}\text{Tc}$ – Tektrotyd
370 - 740 MBq
1,7- 4,5 mSv

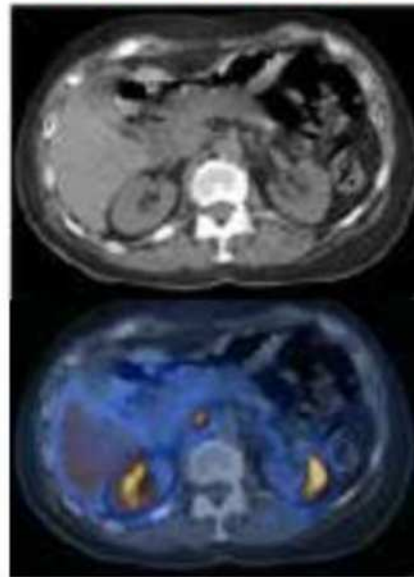
FP: PANCREAS, UNCINATE PROCESS/HEAD

Kuni 1/3 patsientidest

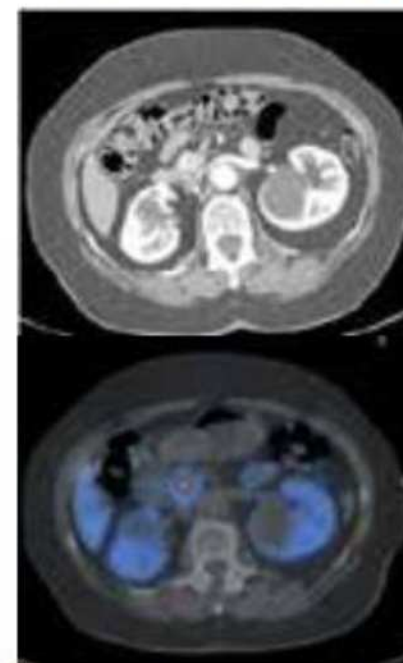
- **DIFFUSE,**
CT NEGATIVE



- **FOCAL,**
CT NEGATIVE



- **FOCAL,**
CT POSITIVE (TP)



Gabriel M et al. J Nucl Med. 2007
Castellucci P et al. J Nucl Med. 2011.

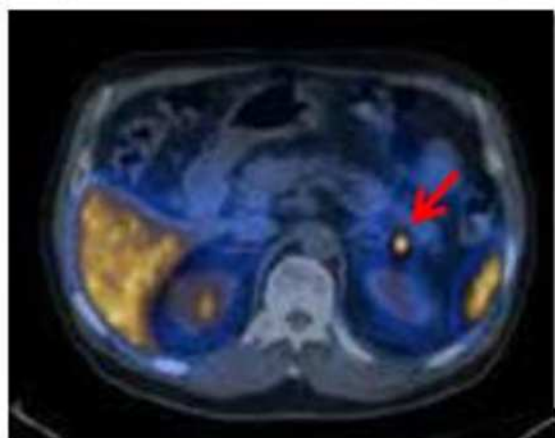
ESMIT

The European School of Multimodality Imaging & Therapy (ESMIT)

(EANM)

EUROPEAN ASSOCIATION OF NUCLEAR MEDICINE

FP: ACCESSORY SPLEENS (AS)



POSTMORTEM STUDIES: approx. 10%
(311/3000pts) show AS
(higher prevalence-60%- after splenectomy or
trauma)

Ludtke FE et al. Acta Chir Scand 1989;155:533-9

Intrapancreatic accessory spleen: **approx
20%** of single AS @ autopsy (54/272 solitary
AS→pancreatic tail)

FP: INFLAMMATION/INFECTION

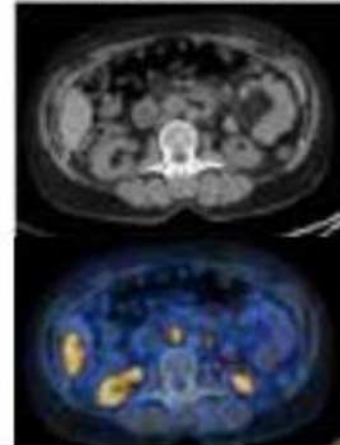
**CHRONIC
GASTRITIS**



SARCOIDOSIS

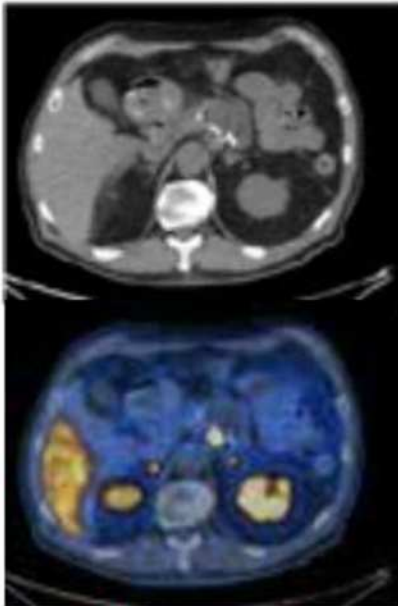


LYMPHOMA



- Osteoblastiline aktiivsus (k.a. vertebraalne hemangioom
- Meningioomid

**CHRONIC
PANCREATITIS**



**positive surgical
margins (ABSCESS)**

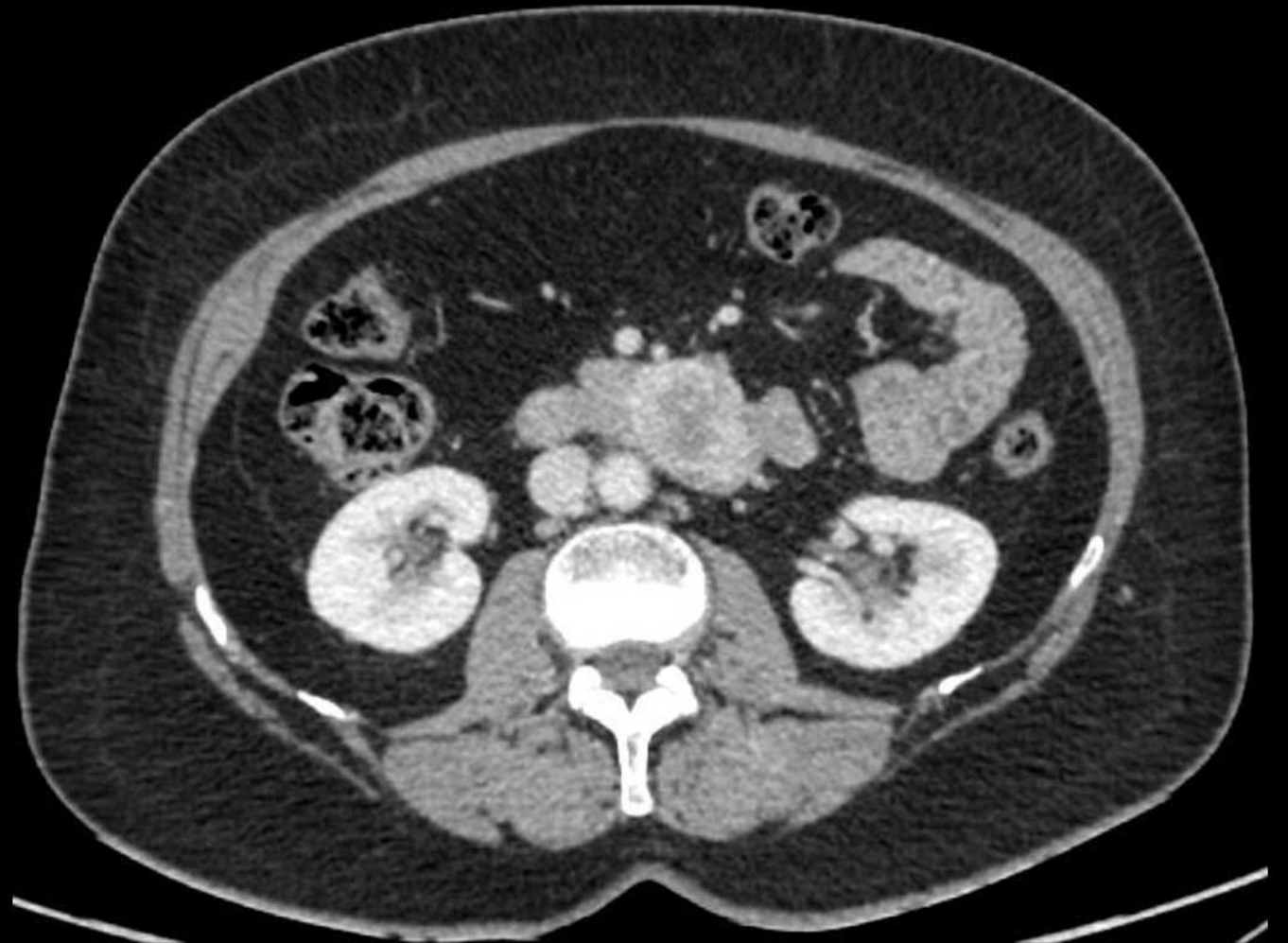


TUBERCULOSIS



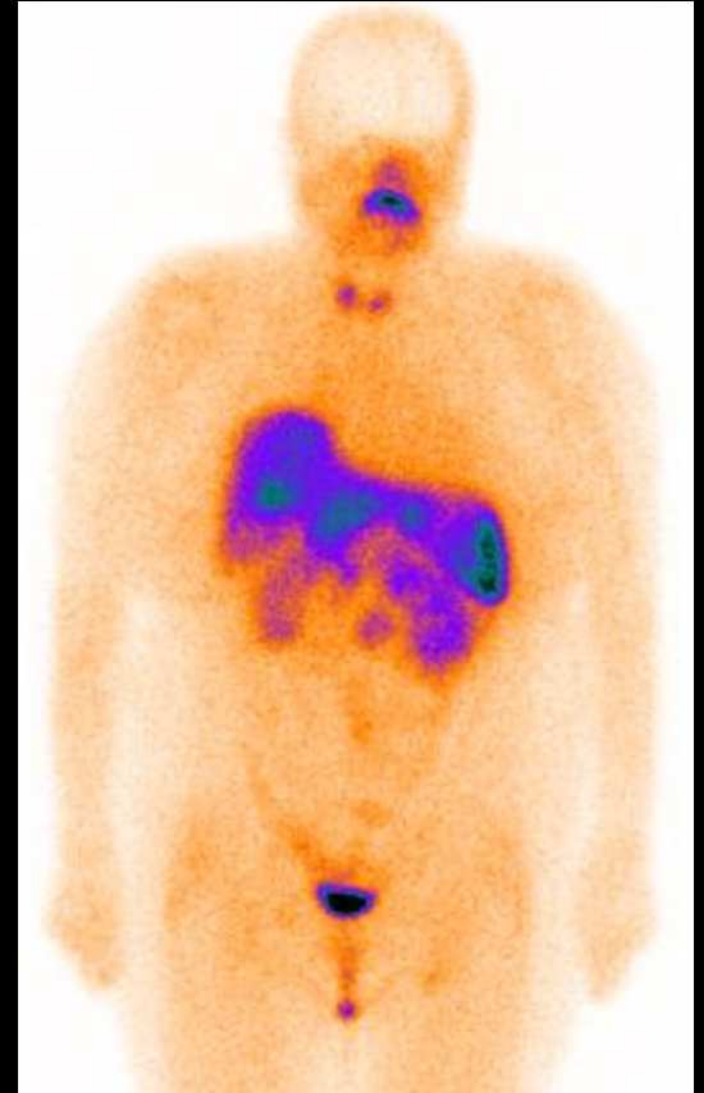
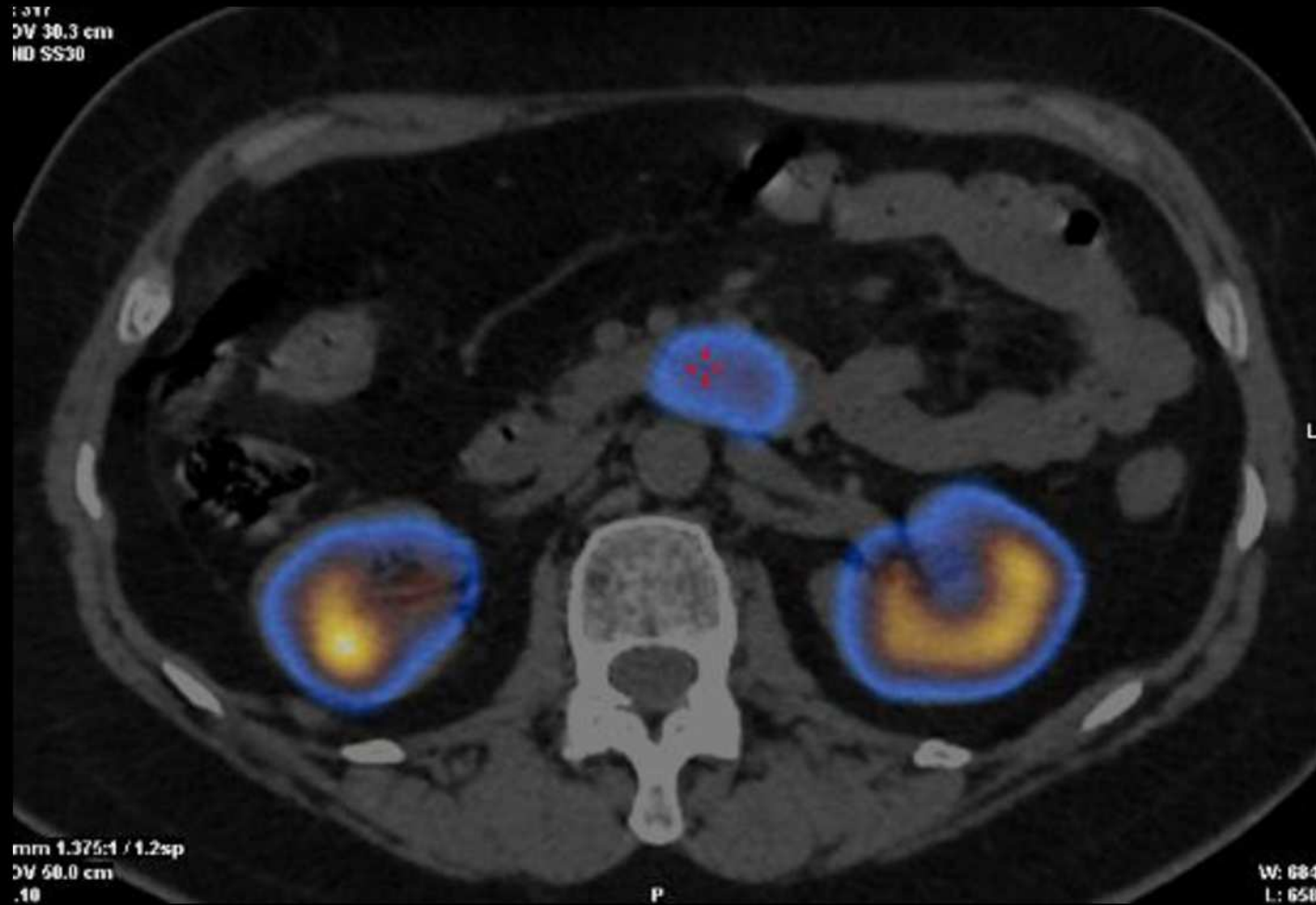
HJ1, N, 1961 a.

Kõhuõõne sonograafial ebaselge lisamass paraaortaalsel



15.09.2019 KT

HJ1 (2) Histo: GIST Ø 3,8 cm : pT2, Ki67 1,15%

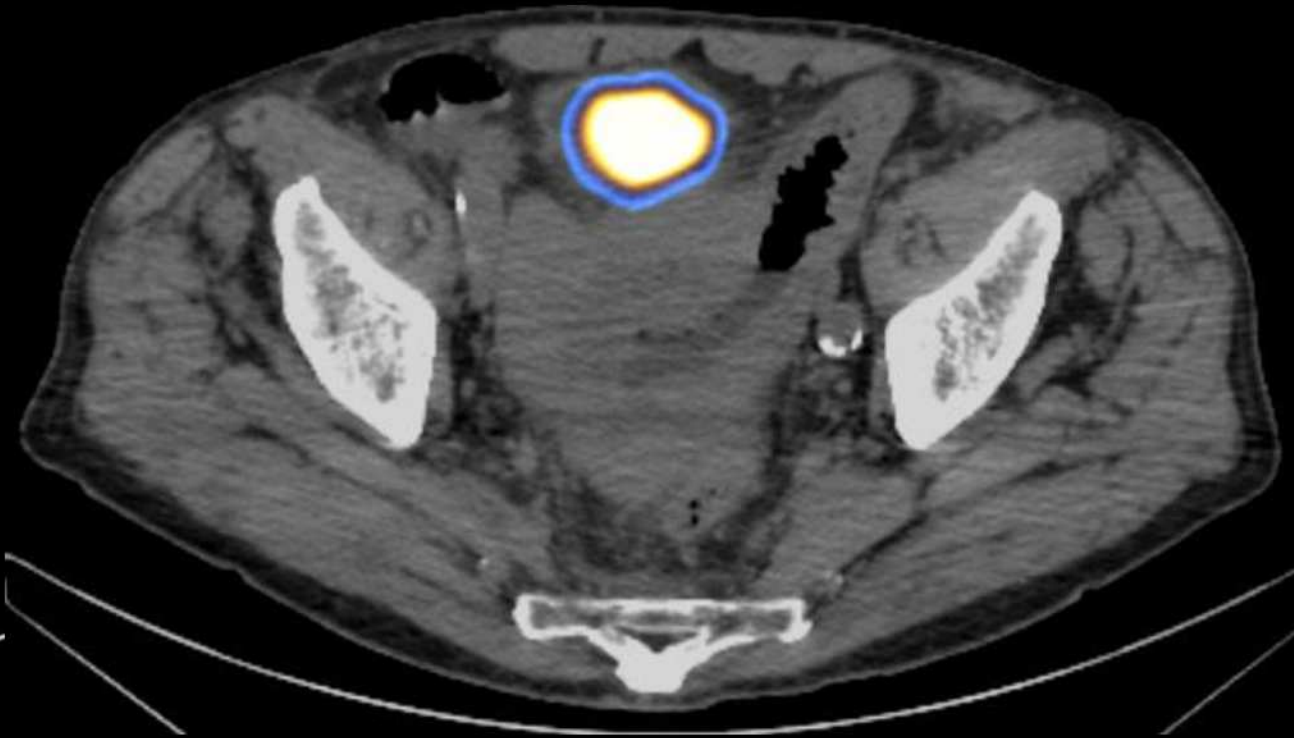


10.10.2019 ^{99m}Tc-Tektrotyd SPET/KT

HJ2, M, 1936 a.
Histo: T-rakkuline lümfoom



16.09.2019 KT



04.11.2019 ^{99m}Tc-Tektrotyd SPET/KT

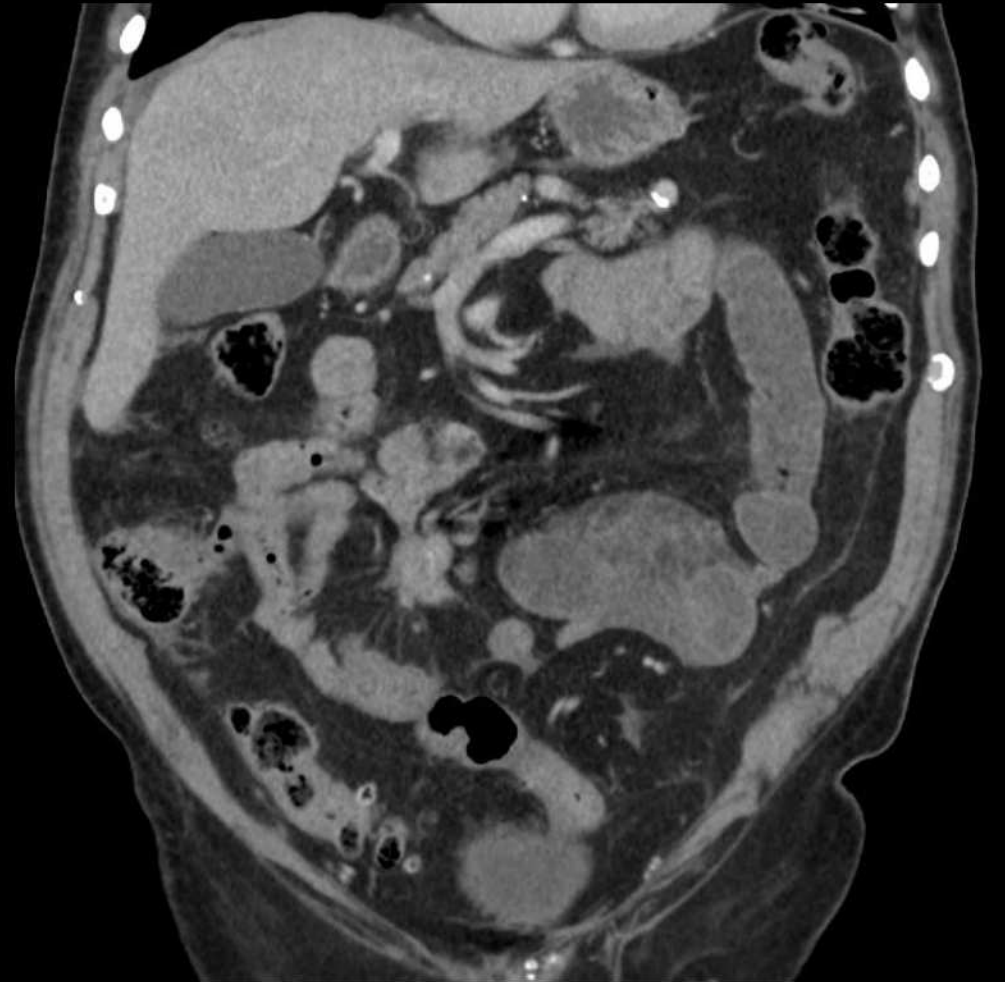
HJ3, M, 1933 a.

Tugev ülakõhuvalu.

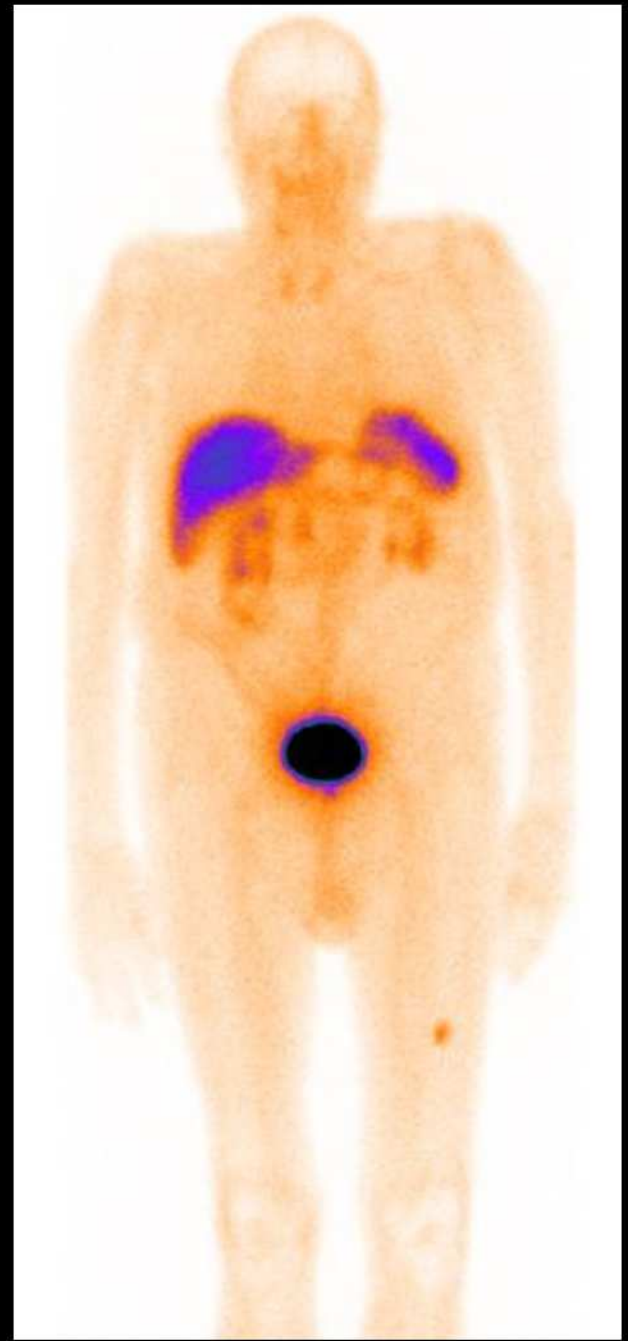
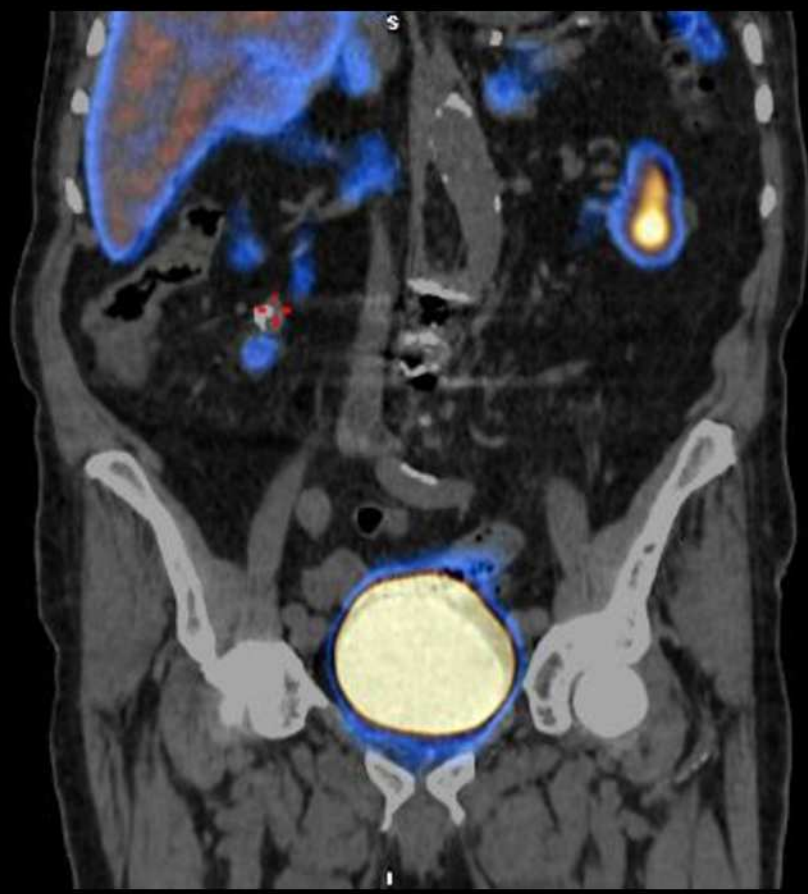
Histo: NET, Grade 2 pT2 N2 PN LVI R0. Ki67 kuni 5%



11.10.2019 KT

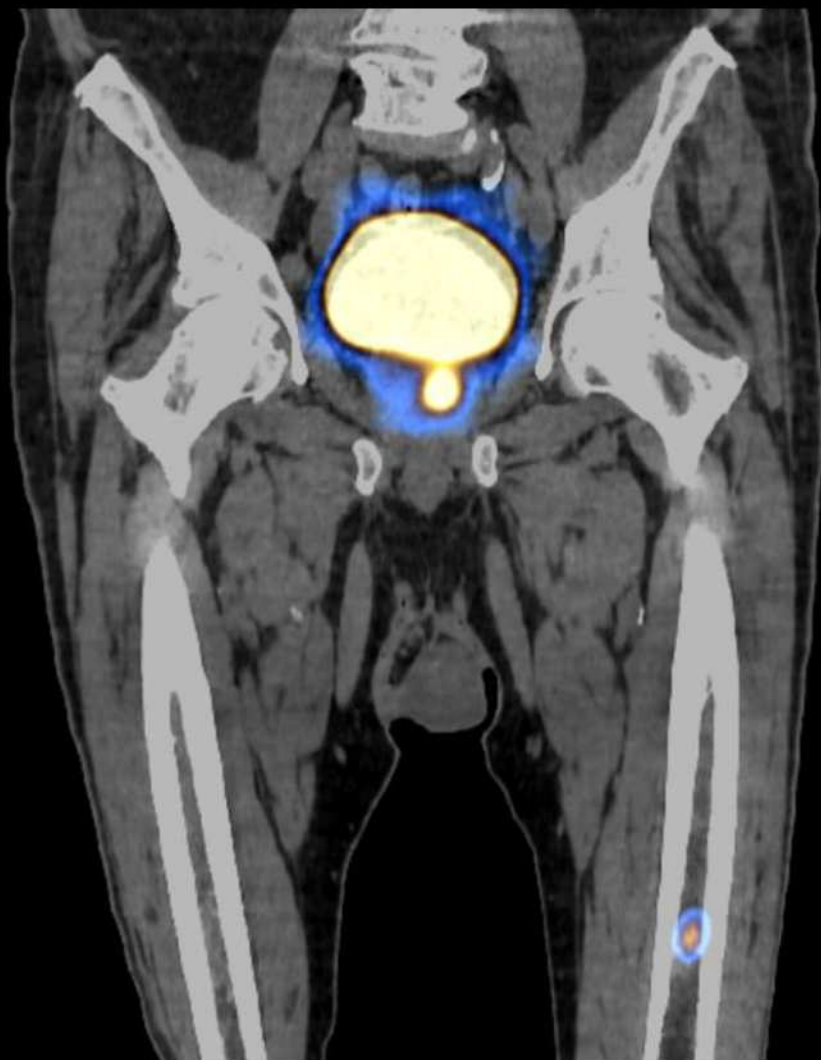


HJ3 (2)



13.11.2019 ^{99m}Tc -Tektrotyd SPET/KT

HJ3 (3)



13.11.2019 ^{99m}Tc -Tektrotyd SPET/KT

HJ4, N, 1995 a.

- 13.07.2017 : Kliiniliselt ning analüüside alusel kahtlus Cushingi tõvele, tõusnud nii AKTH kui ka kortisool - viitab hüpofüüsile adenoomile.
- 18.07 tehtud ka sinus petrosuste kateteriseerimine ja CRH test, mille tulemus viitab AKTH-d sekreteerivale ektoopilisele koldele.
- 08.2017. a. opereeritud vasaku kopsu lingulas paiknevat tüüpilist kartsinoidi G1, millega kaasnes ektoopiline Cushingi sündroom. Selle järgselt hüperkortisolism järk-järgult lahenes.
- 2019 aasta suve lõpust märkas patsient muutusi enesetundes ja välimuses. Tekkis kuunägu, jämenes kael, tekkis ka aknelaadne lööve üle keha, põlvevalud, ärevus, uinumisraskused.

HJ4 (2)

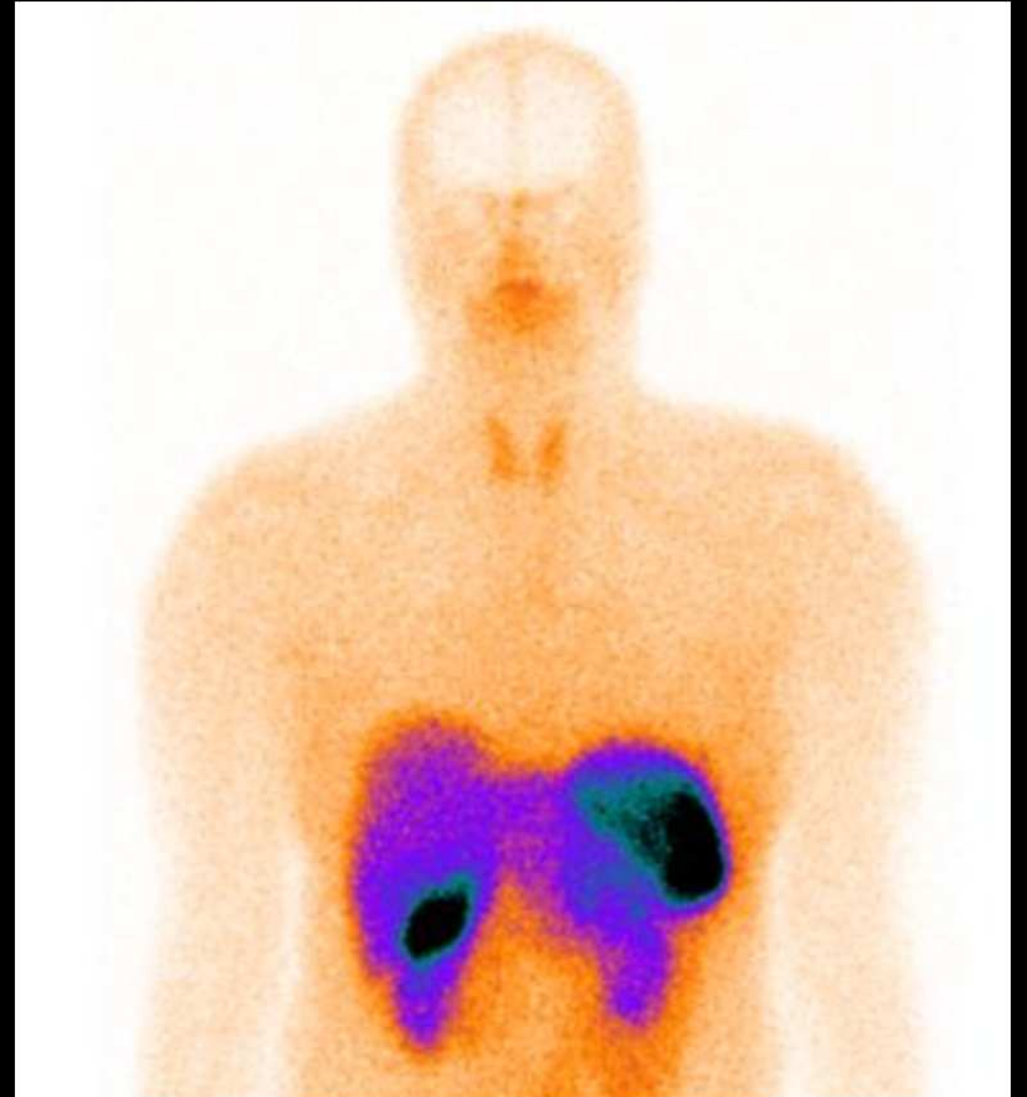
Histo: tüüpiline kartsinoid, G1, pT1b R0. Ki67 1,7 %
AKTH värvingul tugev difuussne positiivne reaktsioon



HJ4(3)

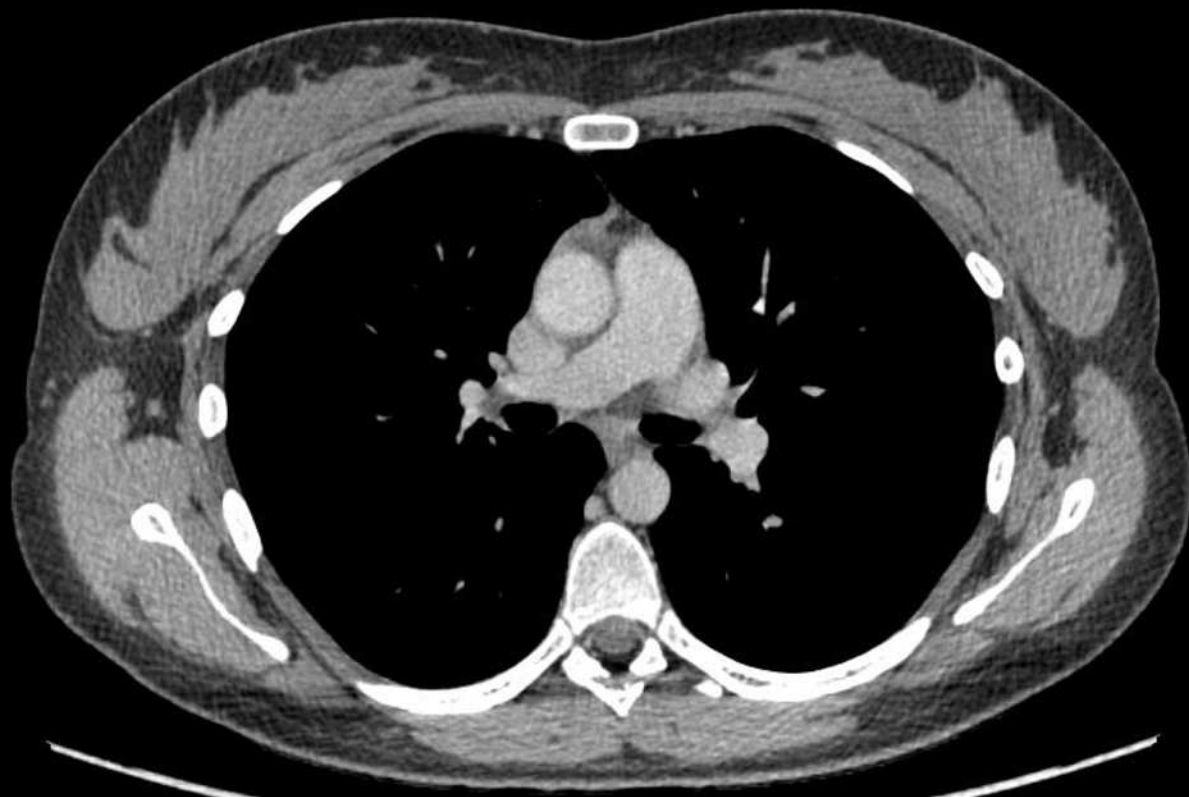
13.03.2019 ja 06.11.2019 KT uuringud leiuta
06.2019 a. tekkinud uuesti kaebused- nägu
muutunud ümaramaks, akne sarnane lööve
näol, kehal kehakaal suurenenud 3kg,
liigesvalud (põlved).

21.10.2019 Kortisool uriinis 5410,7 nmol/d
(N 8,3-118,7)

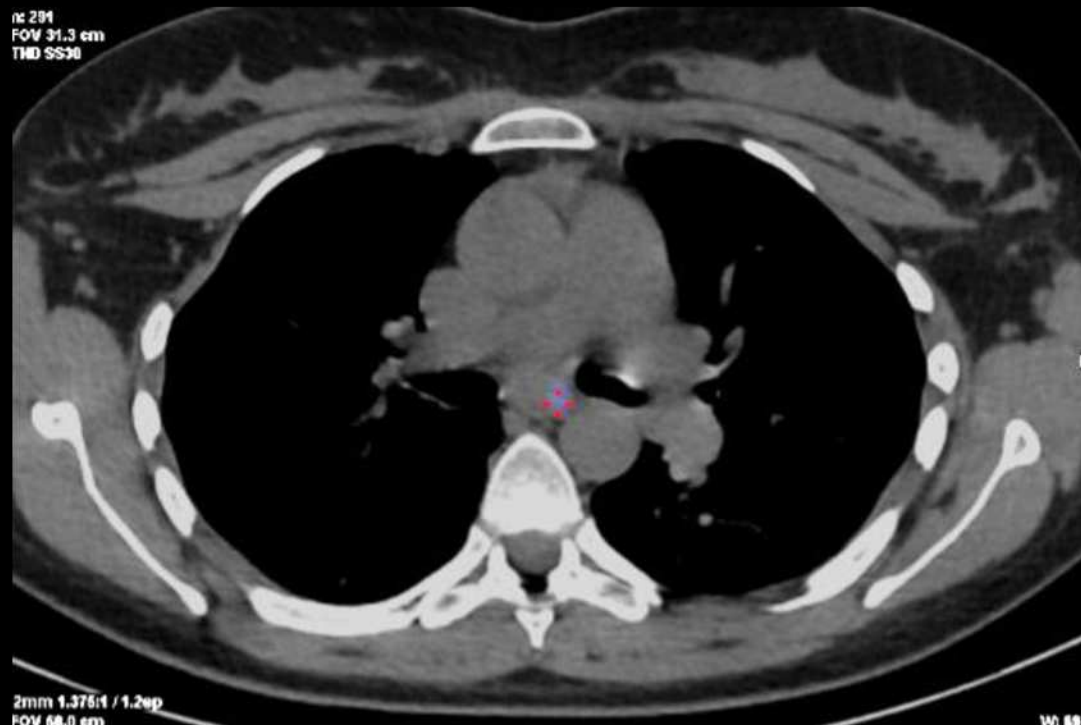


13.11.2019 ^{99m}Tc-Tektrotyd SPET/KT

HJ4 (4)

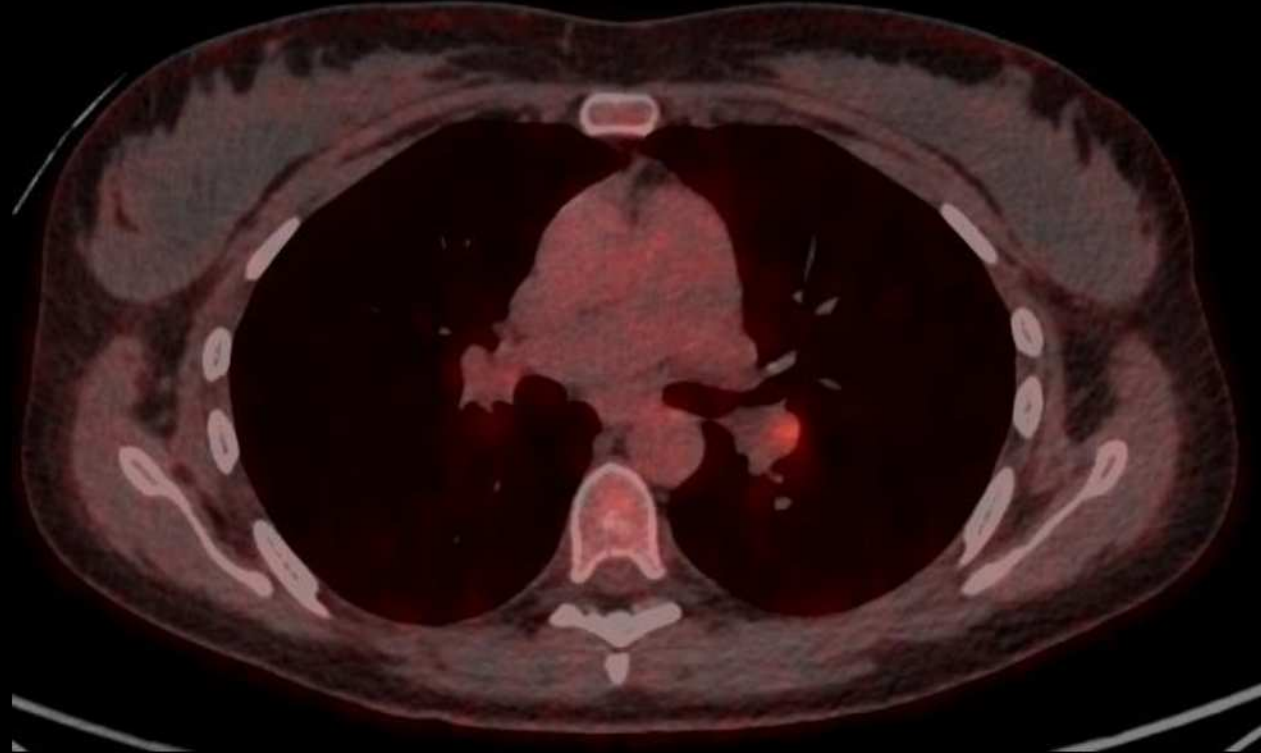


06.11.2019 KT



13.11.2019 ^{99m}Tc-Tektrotyd SPET/KT

HJ4 (5)

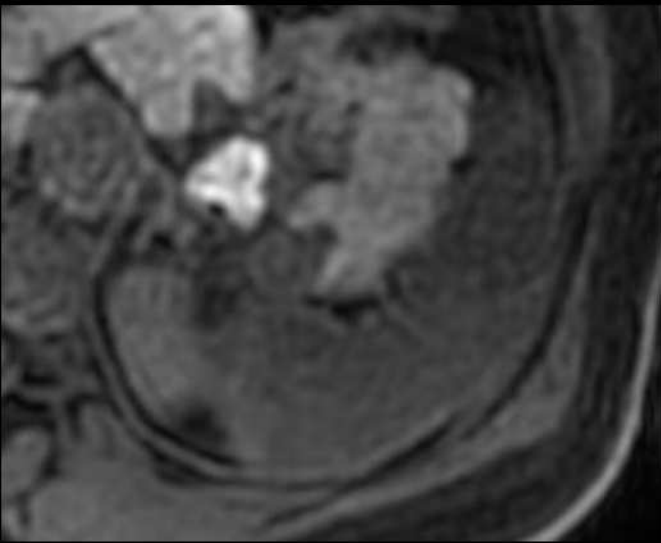


29.11.2019 ^{18}F -FDG PET/CT

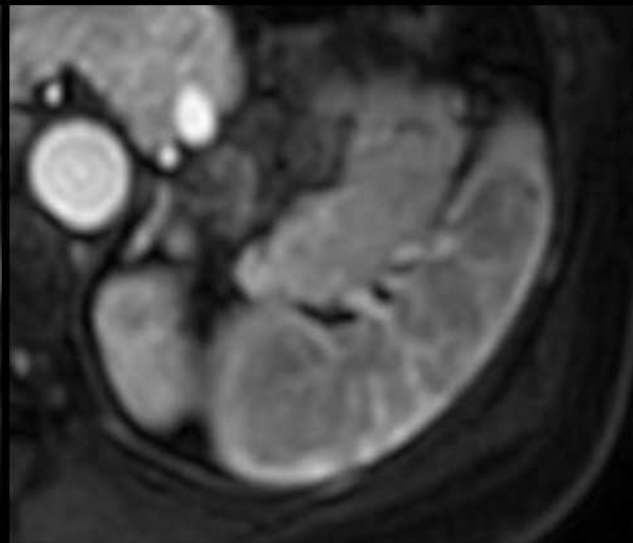
HJ4 (6)

- 27.11.19 hospitaliseeritud, K 2,2 mmol/L
09.12.19 bronhoskoopial: Traheea bif. aluses regioonis vasaku peabronhi mediaalse seinaga on kontaktis kuni 15mm inhomogeensed l/s-d
Keskseinandi lümfisõlmes 7L immuunohistokeemiliselt: CK AE1/AE3, sünaptofüsiin ja kromogranin A positiivne; TTF-1 negatiivne; Ki 67 0,5%. Leid vastab tüüpilise kartsinoidi metastaasile keskseinandi lümfisõlmes.
- 19.12.2019 Lobektoomia sin sup. Lümfadenektoomia regioonidest nr. 4L,5,6,7,8,10R.
- “Pre- ja postoperatiivselt AKTH sündroom, mis suhteliselt stabiilse seisundi foonil kiiresti läinud üle hulgiorganpuudulikkuseks. Põhjustena tulevad arvesse intraparenhümaatoosne verejooks või fulminantne sepsis”.
- Surmlõpe 25.12.2019 kell 12.49. Pata.anat. Lahang.

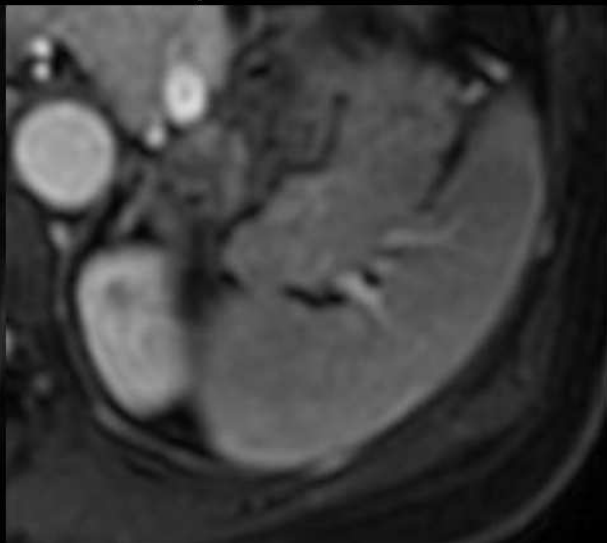
T1 (mDIXON) natiiv



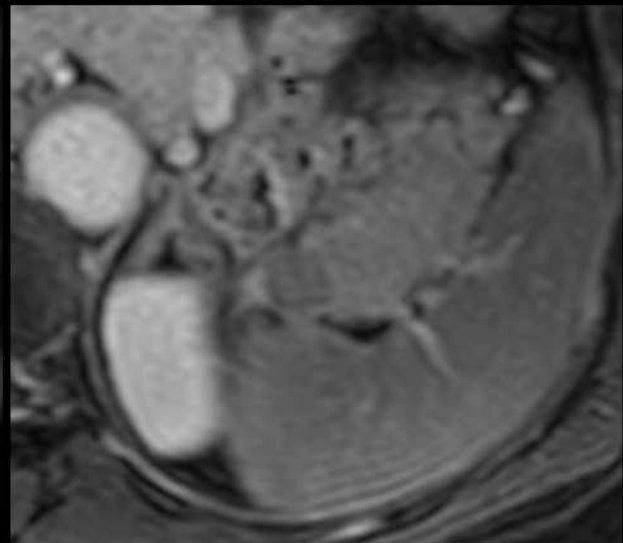
art.



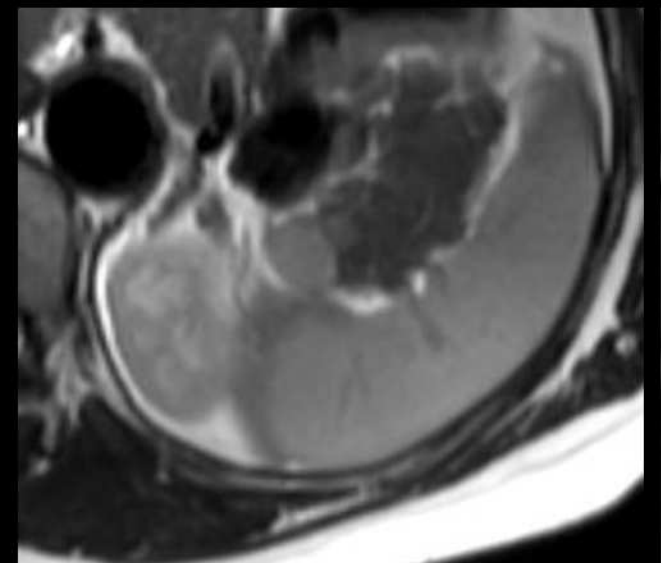
porto-ven.



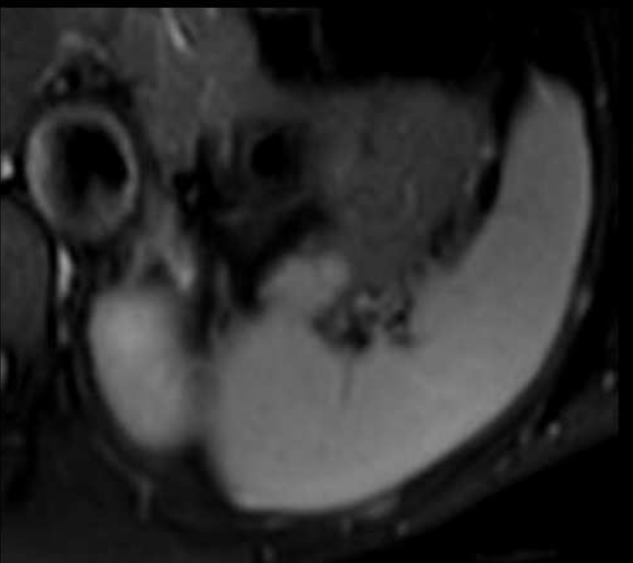
8 min hilis



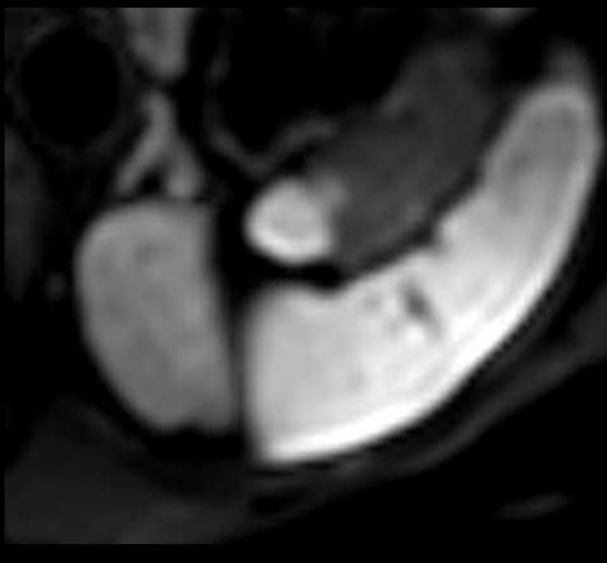
HJ 5, 26.11.2019 ja 29.11.2019 MRT



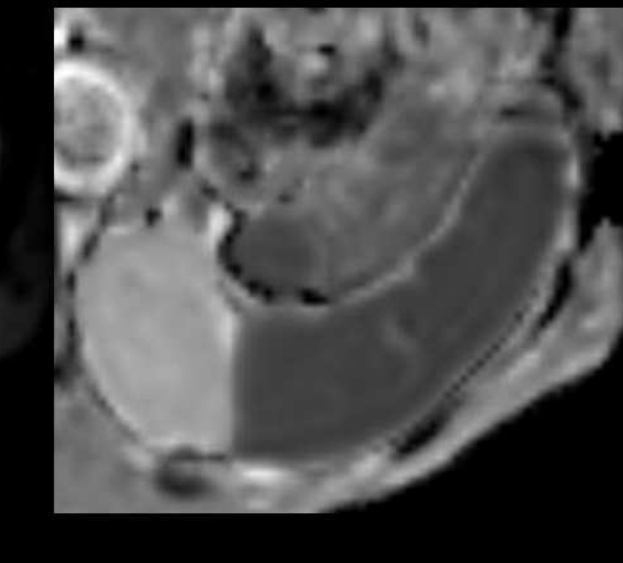
T2



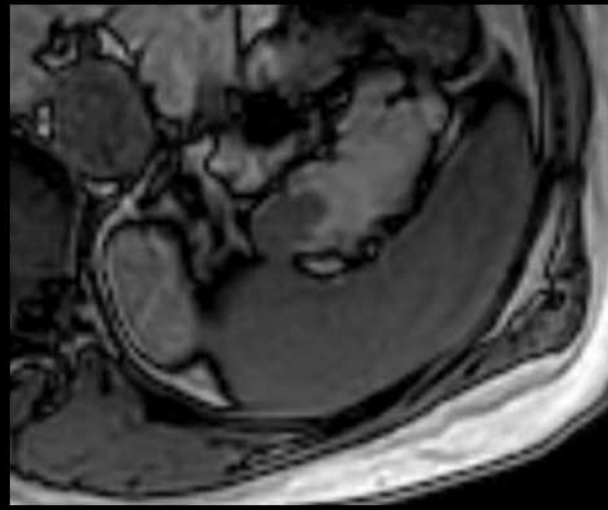
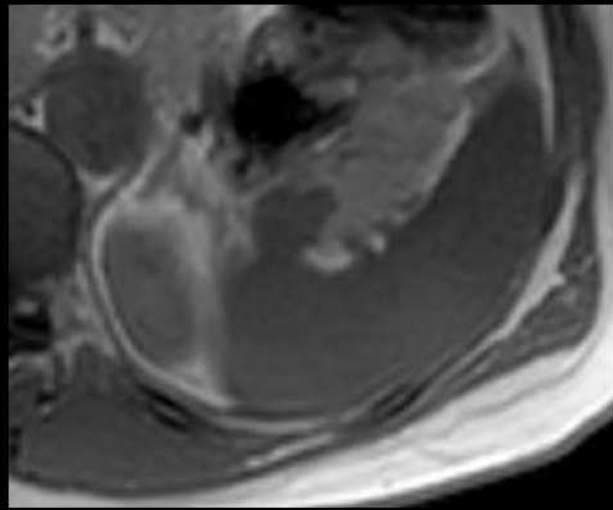
T2 SPAIR



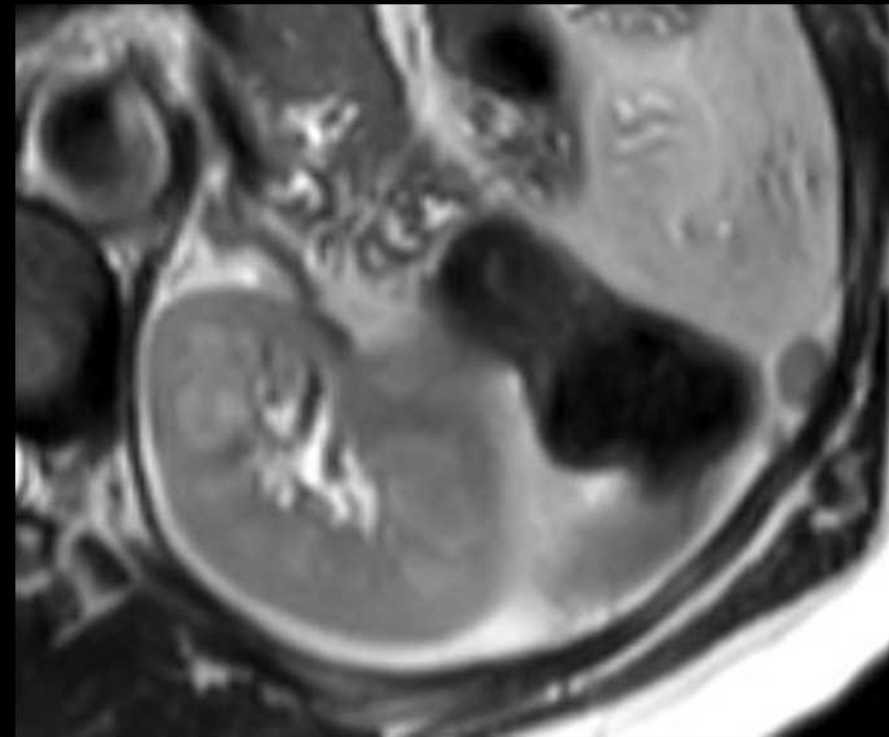
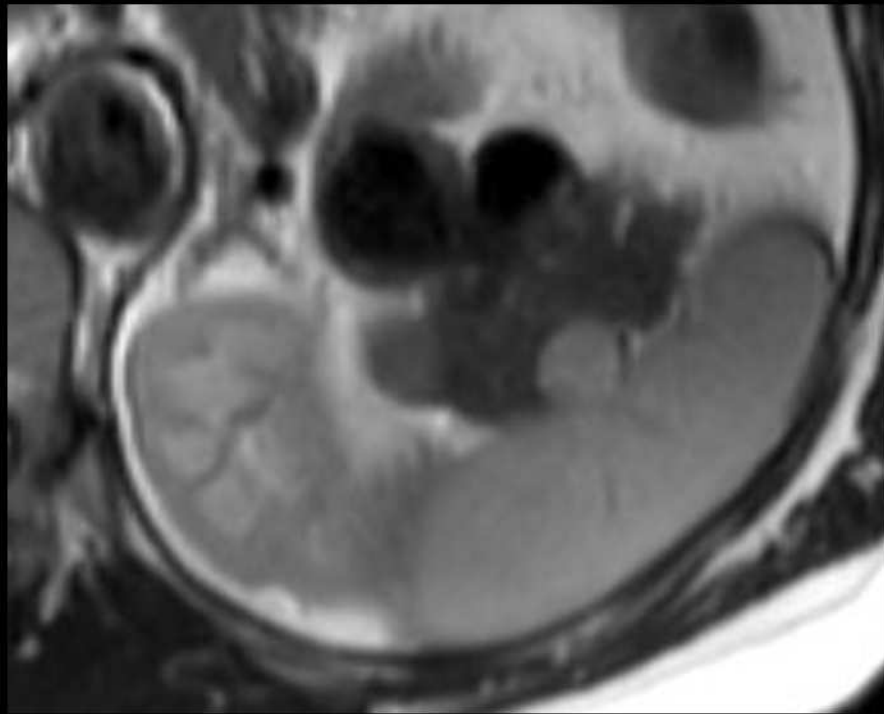
DWI



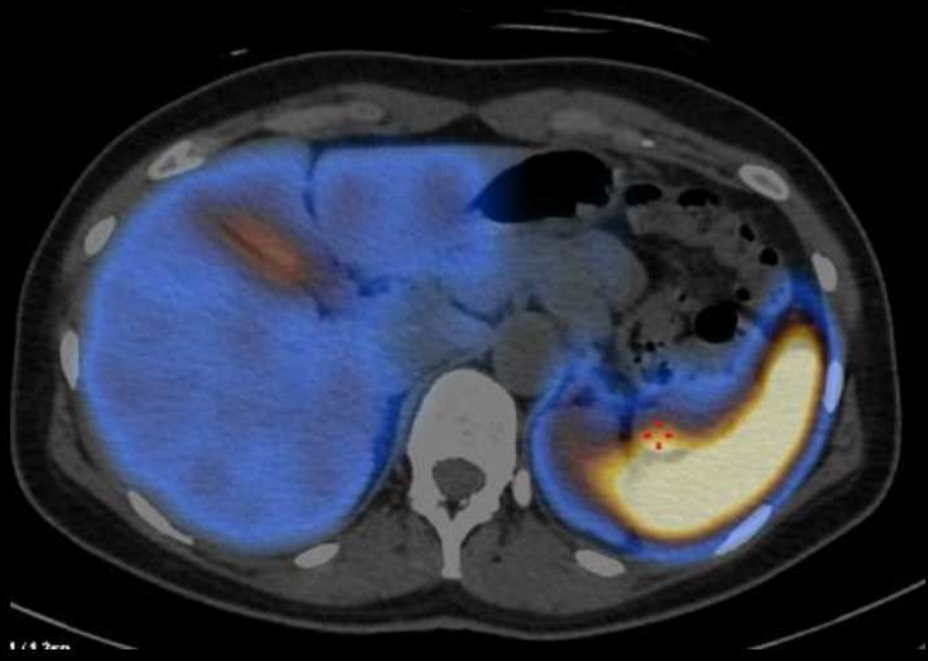
ADC



In-phase and out-of-phase



T2



17.12.2019 99mTc- Tektortyd SPET/KT



16.10.2014 UH

HJ6, N, 1942 a.

- 2015: Haiguse anamnees:
Sattus Pärnu Haiglasse
kõhuvalude tõttu.

Korralikult uuritud, leitud maksas
kolded, punkteeritud NET G2
vastusega, algkollet ei leia –
peensool?

2015 op - Leid sobib peensoole
NET-le, G2, pT3, Ki67 15%.

Ravi: peensoole resektsioon, SSA

2.11.16 - 22.11.17: saanud 5
177Lu-DOTATE ravikuuri, maksa
mts-d stabiilsed



01.08.2015 KT

HJ6 (2)



01.09.2016 KT

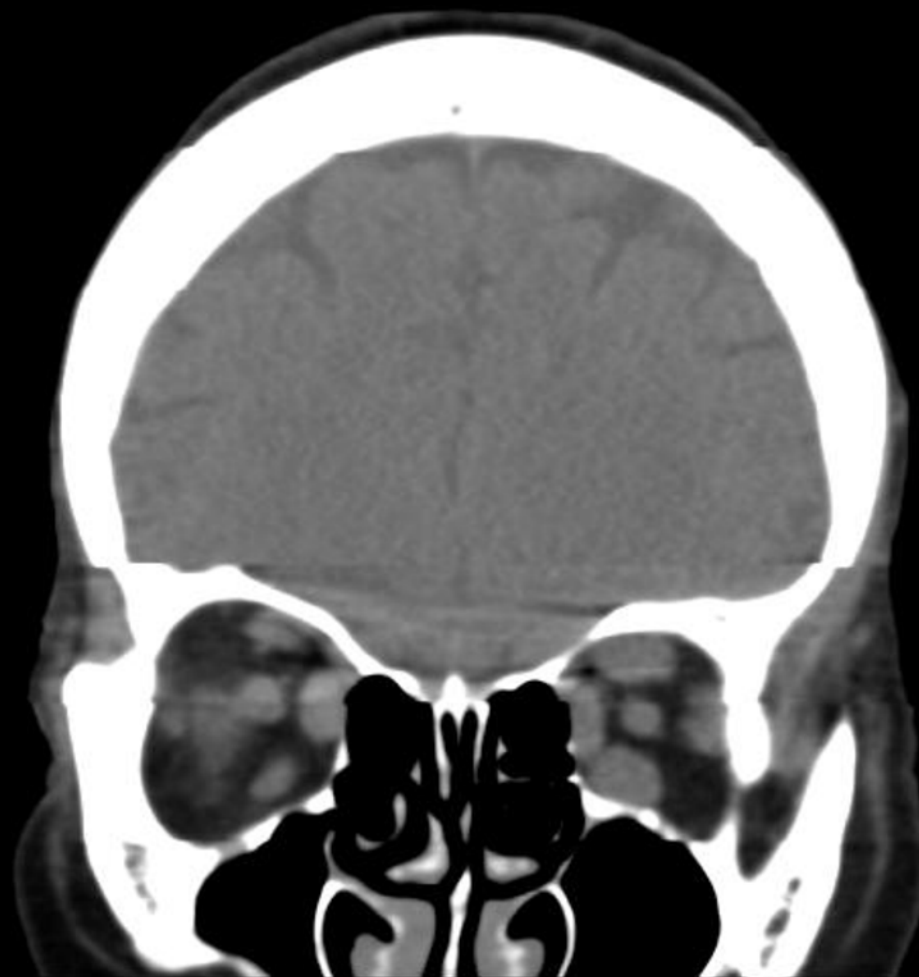


06.03.2018 KT

HJ6 (3)

04.04.2019 KT: Maksa kolded dünaamikas veidi tihedamad, kuid see võib olla kontrasteerumisfaasist tingitud muutus. Tekkinud vähene astsiit.

Paremas rinnas väike sõlm dünaamikas suurenenud - vajadusel täpsustamiseks mammogrammide. Vasaku orbita m. rectus sup. on paremaga võrreldes paksenenud - ebaselge tähendusega leid.



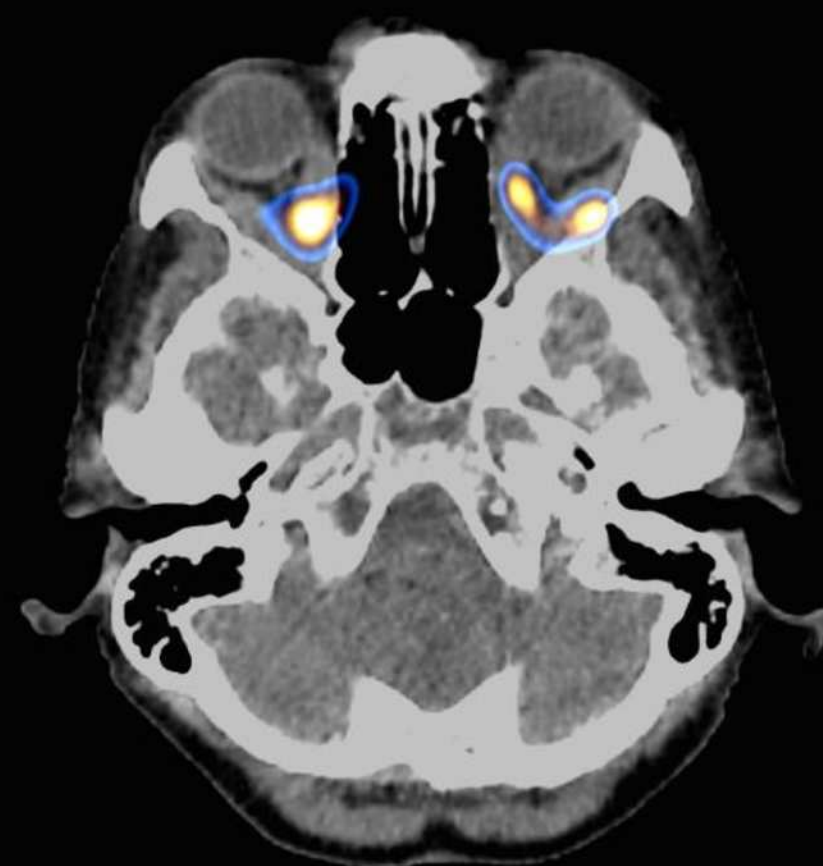
HJ6 (4)



04.04.2019 KT



13.09.2019 KT

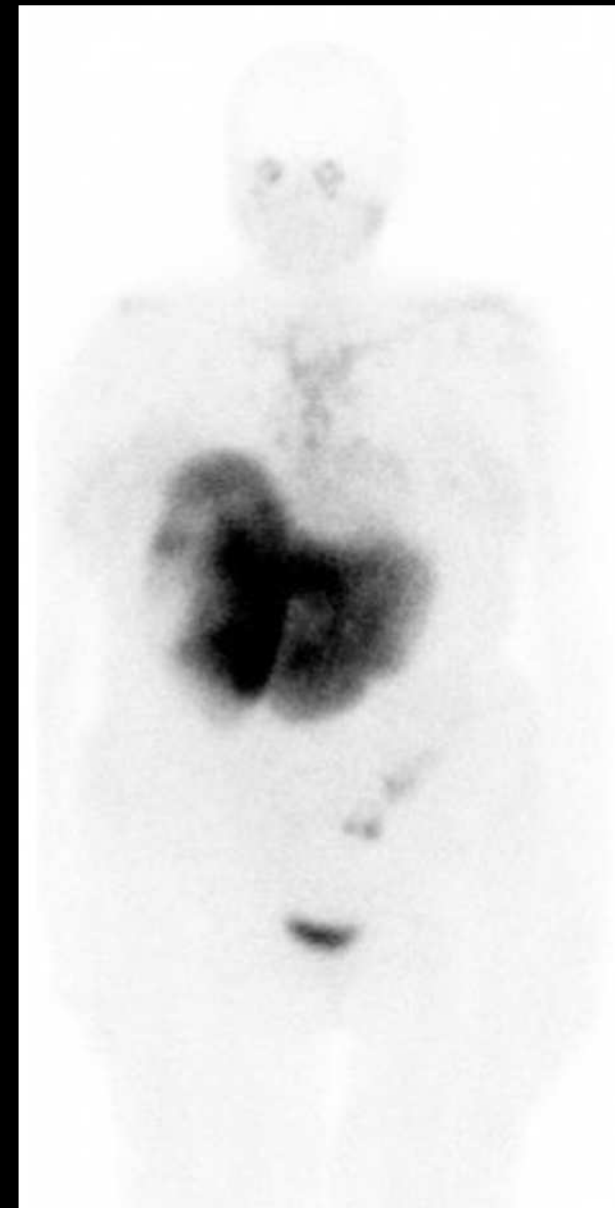
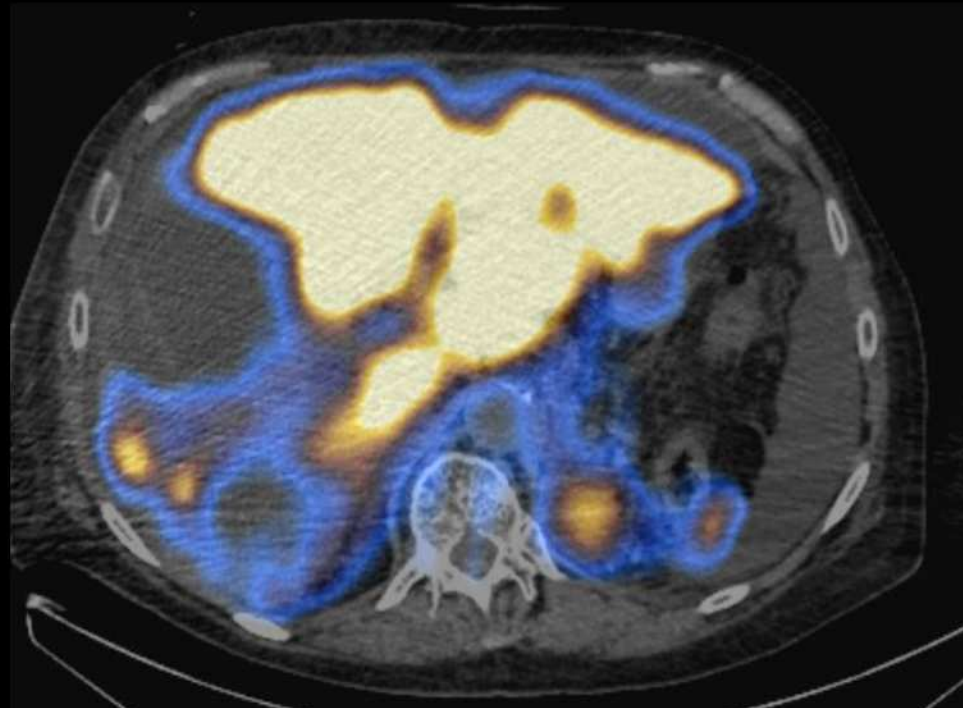
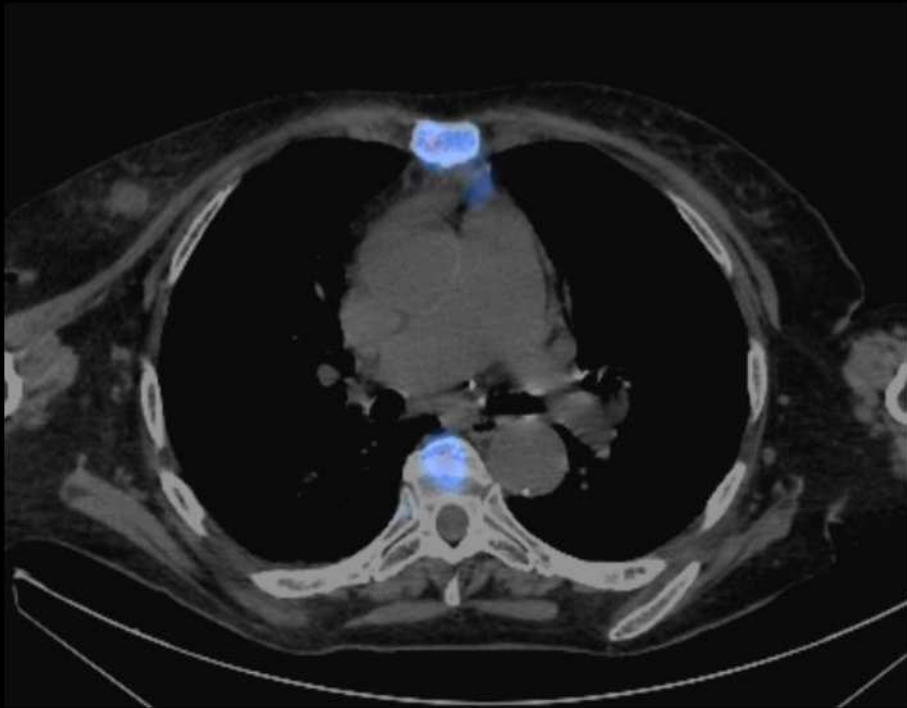


23.09.2019

^{99m}Tc -Tektrotyd SPET/KT

Viimasel ajal lisandunud ka pearinglus, tasakaaluhäire ja kahelinägemine. Maksas rebiopsia Ki67 3%, paremast rinnast algkoldele sobivam 15%; seega G2.

HJ6 (5)



23.09.2019 ^{99m}Tc -Tektrotyd SPET/KT

Kokkuvõte

NET – suhteliselt hea prognoosiga, kuid eluiga lühendav haiguste grupp

PET/KT – „*whenever possible*“

- Parem pildi kvaliteet
- Lühem uuringu aeg (salvestus 60 min post inj.)
- SUVmax kasutamine
- Võimalik madalam kiirgusdoos

Vale positiivsus

- Pankrease pea/proc. uncinatus'es kogunemine
– korrelatsioon KT/MRT-ga

According to The National Geographic Society, the zebra has the most unique coat of all animals. And each individual zebra has its own striped pattern, as unique to it as fingerprints are to humans. In fact, no two are exactly alike. Just like NET patients. No two NET Cancer patients are the same.



CURRENT TRENDS IN NEUROENDOCRINE TUMORS

Have a safe travel back home



Kasutatud kirjandus

- *Dasari A, Shen C, Halperin D, et al. Trends in the Incidence, Prevalence, and Survival Outcomes in Patients With Neuroendocrine Tumors in the United States. JAMA Oncol. 2017;3(10):1335–1342. doi:10.1001/jamaoncol.2017.0589*
- <https://www.uptodate.com/contents/pathology-classification-and-grading-of-neuroendocrine-neoplasms-arising-in-the-digestive-system#H13525387>
- **Lewis RB, Lattin GE et al. Pancreatic Endocrine Tumors: Radiologic-Clinicopathologic Correlation. RadioGraphics 2010 30:6, 1445-1464**
<https://pubs.rsna.org/doi/full/10.1148/rg.306105523>
- *Tamm EP, Bhosale P, Lee JH, Rohren EM. State-of-the-art Imaging of Pancreatic Neuroendocrine Tumors. Surg Oncol Clin N Am. 2016;25(2):375–400. doi:10.1016/j.soc.2015.11.007*
- *Ren S, Chen X, Wang Z, Zhao R, Wang J, Cui W, et al. (2019) Differentiation of hypovascular pancreatic neuroendocrine tumors from pancreatic ductal adenocarcinoma using contrast-enhanced computed tomography. PLoS ONE 14(2): e0211566.*
- *Worhunsky DJ, Krampitz GW, Poullos PD, et al. Pancreatic neuroendocrine tumours: hypoenhancement on arterial phase computed tomography predicts biological aggressiveness. HPB (Oxford). 2014;16(4):304–311.*
- **Baxi AJ, Chintapalli K et al. Multimodality Imaging Findings in Carcinoid Tumors: A Head-to-Toe Spectrum. RadioGraphics 2017 37:2, 516-536:**
<https://pubs.rsna.org/doi/10.1148/rg.2017160113>
- **Jeung MY, Gasser B, et al. Bronchial Carcinoid Tumors of the Thorax: Spectrum of Radiologic Findings. RadioGraphics 2002 22:2, 351-365**
<https://pubs.rsna.org/doi/full/10.1148/radiographics.22.2.g02mr01351>
- *Woodbridge LR, Murtagh BM et al. Midgut Neuroendocrine Tumors: Imaging Assessment for Surgical Resection. RadioGraphics 2014 34:2, 413-426*
- *Bodei L, Sundin A et al. The Status of Neuroendocrine Tumor Imaging: From Darkness to Light? Neuroendocrinology 2015;101:1-17. doi: 10.1159/000367850*
- *Hofman MS, Kong G, Neels OC, Eu P, Hong E, Hicks RJ. High management impact of Ga-68 DOTATATE (GaTate) PET/CT for imaging neuroendocrine and other somatostatin expressing tumours. J Med Imaging Radiat Oncol 2012;56(1):40–47.*
- **Hofman MS, Lau WFE, Hicks RJ. Somatostatin Receptor Imaging with 68Ga DOTATATE PET/CT: Clinical Utility, Normal Patterns, Pearls, and Pitfalls in Interpretation. RadioGraphics 2015 35:2, 500-516**
<https://pubs.rsna.org/doi/full/10.1148/rg.352140164>
- *Pauwels E, Cleeren F, Bormans G, Deroose CM. Somatostatin receptor PET ligands - the next generation for clinical practice. Am J Nucl Med Mol Imaging. 2018;8(5):311–331. Published 2018 Oct 20.*
- *Virgolini I, Ambrosini V, Bomanji JB, Baum RP et al. Procedure guidelines for PET/CT tumour imaging with 68Ga-DOTA-conjugated peptides: 68Ga-DOTA-TOC, 68Ga-DOTA-NOC, 68Ga-DOTA-TATE. Eur J Nucl Med Mol Imaging. 2010 Oct;37(10):2004-10.*
- *Sundin A, Arnold R et al. ENETS Consensus Guidelines for the Standards of Care in Neuroendocrine Tumors: Radiological, Nuclear Medicine & Hybrid Imaging. Neuroendocrinology. 2017;105(3):212-244*